Aeolian Research 2 (2011) 181–204

Contents lists available at ScienceDirect

Aeolian Research

journal homepage: www.elsevier.com/locate/aeolia

Review Article

Dust cycle: An emerging core theme in Earth system science

Yaping Shao [a,*], Karl-Heinz Wyrwoll [b], Adrian Chappell [c], Jianping Huang [d], Zhaohui Lin [e], Grant H. McTainsh [f], Masao Mikami [g], Taichu Y. Tanaka [g], Xulong Wang [h], Soonchang Yoon [i]

[a] Institute for Geophysics and Meteorology, University of Cologne, Cologne, Germany
[b] School of Earth and Environment, The University of Western Australia, WA 6009, Australia
[c] Division of Land and Water, CSIRO, Canberra, Australia
[d] College of Atmospheric Sciences, Lanzhou University, Lanzhou 730000, China
[e] Institute for Atmospheric Physics, Chinese Academy of Sciences, Beijing, China
[f] Atmospheric Environment Research Centre, Griffith University, Brisbane, Australia
[g] Meteorological Research Institute, Japan Meteorological Agency, Tsukuba, Japan
[h] Institute of Earth Environment, Chinese Academy of Sciences, X'ian 710075, China
[i] School of Earth and Environmental Sciences, Seoul National University, Seoul, South Korea

ARTICLE INFO

Article history:
Received 23 May 2010
Revised 3 February 2011
Accepted 3 February 2011

Keywords:
Dust
Dust cycle
Aeolian processes
Energy cycle
Carbon cycle
Climate change

ABSTRACT

The dust cycle is an integral part of the Earth system. Each year, an estimated 2000 Mt dust is emitted into the atmosphere, 75% of which is deposited to the land and 25% to the ocean. The emitted and deposited dust participates in a range physical, chemical and bio-geological processes that interact with the cycles of energy, carbon and water. Dust profoundly affects the energy balance of the Earth system, carries organic material, contributes directly to the carbon cycle and carries iron which is vital to ocean productivity and the ocean-atmosphere CO_2 exchange. A deciphering of dust sources, transport and deposition, requires an understanding of the geological controls and climate states – past, present and future. While our knowledge of the dust cycle, its impacts and interactions with the other global-scale bio-geochemical cycles has greatly advanced in the last 30 years, large uncertainties and knowledge gaps still exist. In this review paper, we attempt to provide a benchmark of our present understanding, identify the needs and emphasise the importance of placing the dust issue in the Earth system framework. Our review focuses on (i) the concept of the dust cycle in the context of global biogeochemical cycles; (ii) dust as a climate indicator; (iii) dust modelling; (iv) dust monitoring; and (v) dust parameters. The adoption of a quantitative and global perspective of the dust cycle, underpinned by a deeper understanding of its physical controls, will lead to the reduction of the large uncertainties which presently exist in Earth system models.

Abbreviations: ACE-Asia, aerosol characterization experiments-Asia; AERONET, aerosol robotic network; AI, aerosol index; AMMA, African Monsoon Multidisciplinary Analysis; AOD, aerosol optical depth; CALIOP, Cloud-Aerosol LIdar with Orthogonal Polarization; CALIPSO, Cloud-Aerosol Lidar and Infrared Pathfinder Satellite Observations; C-cycle, carbon cycle; CCN, cloud condensation nuclei; CERES, clouds and the earth's radiant energy system; BOA, bottom of atmosphere; D-cycle, dust cycle; D–O, Dansgaard–Oescher; ECMWF, European Centre for Medium-Range Weather Forecasts; E-cycle, energy cycle; ERBE, Earth Radiation Budget Experiment; 4DVAR, 4-Dimensional VARiational data assimilation; GALION, Global Atmosphere watch aerosol Lidar Observation Network; GCM, global circulation model; GIPS2, Greenland Ice Sheet Project 2; GIS, Geographical Information System; HNLC, High-Nitrate and Low Chlorophyll; IN, ice nuclei; IPCC, Intergovernmental Panel on Climate Change; ISCCP, International Satellite Cloud Climatology Project; ITD, inter tropical discontinuity; JADE, Japan–Australia Dust Experiment; LGM, last glacial maximum; LNLC, low-nitrate and low-chlorophyll; MASINGAR, Model for Aerosol Species In the Global Atmosphere; MODIS, Moderate Resolution Imaging Spectroradiometer; OMI, Ozone Monitoring Instrument; OSL, optically stimulated luminescence; QEMSCAN, Quantitative Evaluation of Minerals by SCANning electron microscopy; RAMS/CFORS, regional atmospheric modelling system/chemical forecast system; RegCM3, Regional Climate Model version 3; SAMUM, Saharan Mineral Dust Experiment; SDZ, Sahel dust zone; SOC, soil organic carbon; SSA, Single-Scattering Albedo; TOA, top of atmosphere; TOMS, Total Ozone Mapping Spectrometer; TSP, total suspended particulates; WMO, World Meteorological Organization.

* Corresponding author.
E-mail addresses: yshao@uni-koeln.de (Y. Shao), wyrwoll@cyllene.uwa.edu.au (K.-H. Wyrwoll), adrian.chappell@csiro.au (A. Chappell), hjp@lzu.edu.cn (J. Huang), lzh@mail.iap.ac.cn (Z. Lin), g.mctainsh@griffith.edu.au (G.H. McTainsh), mmikami@mir-jma.go.jp (M. Mikami), yatanaka@mri-jma.go.jp (T.Y. Tanaka), wxl@loess.llqg.ac.cn (X. Wang), yoon@snu.ac.kr (S. Yoon).

1875-9637/$ - see front matter © 2011 Published by Elsevier B.V.
doi:10.1016/j.aeolia.2011.02.001

Contents

1. Introduction

Dust as an aerosol significantly impacts on the energy balance of the Earth system through the absorption and scattering of radiation in the atmosphere and the modifications of the optical properties of clouds and snow/ice surfaces. Its importance in the Earth system has been emphasised by the IPCC 4th Assessment Report (IPCC, 2007) which highlighted the net global cooling effect of aerosols that in part, compensates for the global warming effect of the greenhouse gases. But the role of dust in the Earth system extends well beyond its impact on the radiation balance, and involves the interactions with other physical, chemical and biogeochemical processes on global scales. Each year, about 2000 Mt dust is emitted into the atmosphere, of which 1500 Mt is deposited to the land and 500 Mt to the ocean (Tables 2, 3 and 5). In this process, dust carries organic matter and contributes directly to the carbon cycle and transports iron that is vital to ocean productivity and ocean-atmosphere CO_2 exchange. Thus, as Fig. 1 illustrates, the cycles of energy (E-cycle), carbon (C-cycle) and dust (D-cycle) in the Earth system are closely inter-related.

In recent years, the dust processes have become core research subjects in Earth system studies. However, gapes remain in our

Table 1
Estimates of global dust emission in Mt yr^{-1}.

Source	Africa	Asia	America	Australia	Global	Comment
Peterson and Junge (1971)					500	Note 1
D'Almeida (1987)					1900	Note 2
Duce et al. (1991)					>910	Note 3
Tegen and Fung (1994)					3000	Model, 0.1–50 μm
Takemura et al. (2000)					3321	Model, 0.2–20 μm
Werner et al. (2002)	693	197		52	1060	Model, 0.2–44 μm
Tegen et al. (2002)					1700	Model 0.2–44 μm
Chin et al. (2002)					1650	Model 0.2–12 μm
Luo et al. (2003)	1114	173		132	1654	Model 0.1–10 μm
Zender et al. (2003)	980	415	43	37	1490	Model 0.1–10 μm
Ginoux et al. (2004)	1430	496	64	61	2073	Model, 0.1–6 μm
Miller et al. (2004)	517	256	53	148	1019	Model, 0.2–16 μm
Tanaka and Chiba (2006)	1150	575	46	106	1877	Model, 0.2–20 μm

Note 1: estimates based on average concentration and residence time; *Note 2:* budget model and sun photometer aerosol-turbidity data for particles smaller than 5 μm; *Note 3:* deposition of mineral aerosol to ocean.

Table 2
Dust deposition to the ocean from [a]Duce et al. (1991), [b]Prospero (1999), [c]Ginoux et al. (2001), [d]Zender et al. (2003), [e]Tegen et al. (2004), [f]Luo et al. (2003) and [g]Jickells et al. (2005).

Ocean	Dry[a] ($g\ m^{-2}\ yr^{-1}$)	Wet[a] ($g\ m^{-2}\ yr^{-1}$)	Total[a] ($Mt\ yr^{-1}$)	Total[b] ($Mt\ yr^{-1}$)	Total[c] ($Mt\ yr^{-1}$)	Total[d] ($Mt\ yr^{-1}$)	Total[e] ($Mt\ yr^{-1}$)	Total[f] ($Mt\ yr^{-1}$)	Total[g] ($Mt\ yr^{-1}$)
North Pacific	1.5	3.8	480	96	92	31	56	35	72
South Pacific	0.13	0.23	39	8	28	8	11	20	29
North Atlantic	2.9	1.1	220	220	184	178	259	230	202
South Atlantic	0.2	0.27	24	5	20	29	35	30	17
North Indian	2	5.1	144	29	154	48	61	113	118
South Indian	0.22	0.6							
Global total					1814	1490	1800	1650	1790

Table 3
Dry and wet depositions of dust in spring at various locations in China and over the East China Sea. Mean-deposition fluxes are reported in $g\ m^{-2}\ mon^{-1}$, with the range of variations given in parentheses (data from Gao et al. (1997).

Location	Dry	Wet	Total
Xian (38°N, 105°E)	19(3.7–33)	6.0(1.2–11)	25(4.9–44)
Beijing (40°N, 116°E)	15(5.1–51)	3.3(1.2–12)	18(6.3–63)
Qingdao (36°N, 120°E)	1.9(.33–6.9)	1.1(.19–4.2)	3.0(.52–11.1)
Xiamen (24°N, 118°E)	1.1(.33–2.9)	2.5(.57–6.9)	3.6(.90–9.8)
EChi–naSea (28–32°N, 122–13°E)	1.3(.36–2.4)	1.4(.39–2.7)	2.7(.75–5.1)
Baotou (41°N, 110°E)	32	6.9	39
Lanzhou (36°N, 104°E)	35	5.9	41
Kato, HK (23°N, 113°E)	0.42(.061–2.2)	0.96(.14–5)	1.4(.21–7.2)
Kenting, TW (23°N, 12°E)	0.17(.005–1.1)	0.38(.02–3.8)	–
Cheju, SKorea (33°N, 127°E)	1.5(.44–4.3)	1.7(.51–4.9)	3.2(.95-9.2)
Mallipo, SKorea (37°N, 128°E)	1.6(.39–16)	2.1(.93–37)	3.7(1.3–53)

understanding of the driving processes, their interactions and the magnitudes of the fluxes involved in the dust cycle. These uncertainties considerably weaken the explanatory powers of Earth system models. Only with a more adequate representation of the dust cycle, can the necessary veracity be imparted to these models, so as to enable them to capture the overall functioning of the Earth system.

Traditionally, dust was mainly the subject of geomorphologists and geologists, but the last 30 years have seen a dramatic expansion of the dust research frontiers with the establishment of a diverse research community recognising the far-reaching implications of dust to the global environment. Dust research has stimulated the integration of disciplines, including geomorphology, soil physics, meteorology, fluid dynamics, air chemistry and ocean biology. It has also involved diverse methodologies, ranging from field campaigns, Geographical Information System (GIS) analyses, remote sensing numerical modeling, data assimilation as well as field and laboratory experiments.

The importance of dust cycle and the role of dust in the Earth system have been increasingly recognized in the scientific community, as clearly reflected in the recent review paper of Kohfeld and Tegen (2007), Mahowald et al. (2009) and Maher et al. (2010). These reviews well documented some of the advancement in dust research from different perspectives. Kohfeld and Tegen (2007) put forward the concept of dust cycle and examined the role of dust in the Earth system from the view point of past and present dust record. Mahowald et al. (2009) provided a detailed review on dust iron deposition, while Maher et al. (2010) examined the global link between dust, climate and ocean biogeochemistry at the present day and at the last glacial maximum. In this paper, we attempt to further the dust cycle concept and to provide a review on the role of dust in the Earth system as well as dust modeling and monitoring. We shall first introduce the concept of dust cycle and then focus on the relations between the D-cycle and E-cycle and D-cycle and C-cycle, and summarize the recent progresses in dust modeling and monitoring. In each of these sections, we highlight progresses and challenges. These will be further discussed in a series of companion papers that will provide in-depth discussions of specific aspects that can only be provided as an outline in this review.

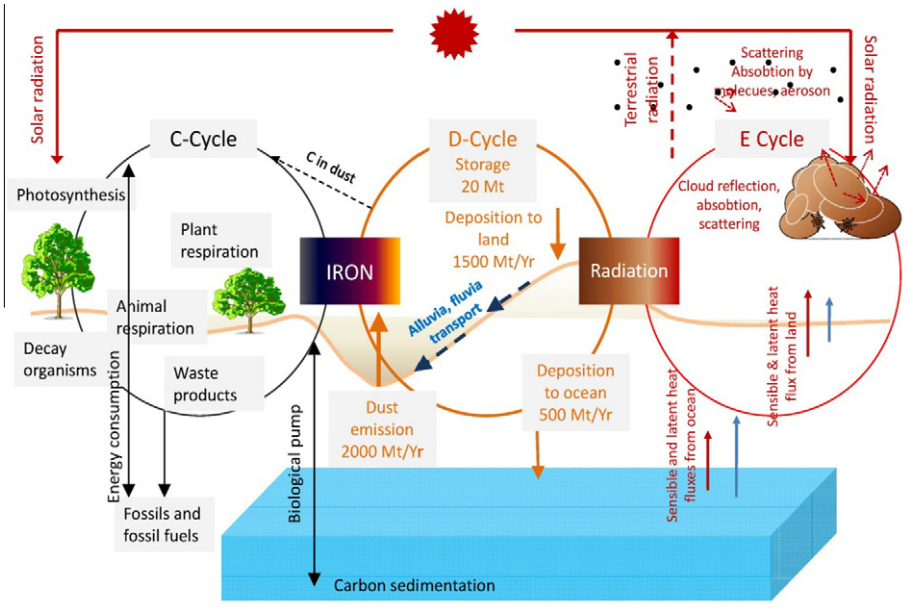

Fig. 1. Links between the dust cycle (D-Cycle) with the carbon cycle (C-Cycle) and the energy cycle (E-Cycle) in the Earth system.

2. Dust cycle, sources, sinks and transport patterns

2.1. Concept of the dust cycle

The dust cycle involves dust emission, transport, transformation, deposition and stabilisation (Fig. 2), but it is not completed on a single time scale. Like the carbon cycle, it involves a range of processes which occur on spatial scales from local to global and on time scales from seconds to millions of years. Taking a global dust cycle approach allows the establishment of the linkages between the terrestrial settings, the atmosphere and the marine biosphere, which then brings to light the internal forcings and feedbacks within the Earth system provoked by dust processes and events (Steffen et al., 2004).

The delivery of dust from source to sink is spatially and temporally discontinuous (e.g., processing of previously stored aeolian and other sediments exposed by land-use change). A summary of the processes involved, with spatial and temporal scales, is given in Fig. 3. As shown, dust is entrained into the atmosphere at the micro-scale by wind shear and turbulence. Once airborne, dust is carried by turbulence and convection to the upper levels of the atmosphere and then transported by synoptic and global circulations over a range of distances. Dust particles also react and mix with anthropogenic air pollutants, which intercept and reflect atmospheric radiation and create cloud condensation nuclei (CCN). They are eventually returned to the surface somewhere downwind by dry and/or wet deposition (Fig. 2, Tables 1, 2 and 4).

Fig. 3 further shows that dust emission, transport and deposition are fast processes in the dust cycle, with time scales ranging from seconds to years. In contrast, the formation of dust sources and the stabilisation of dust deposits are much longer-term processes which involve weathering and soil formation, creation of alluvial and other sediment registers and subsequent emission

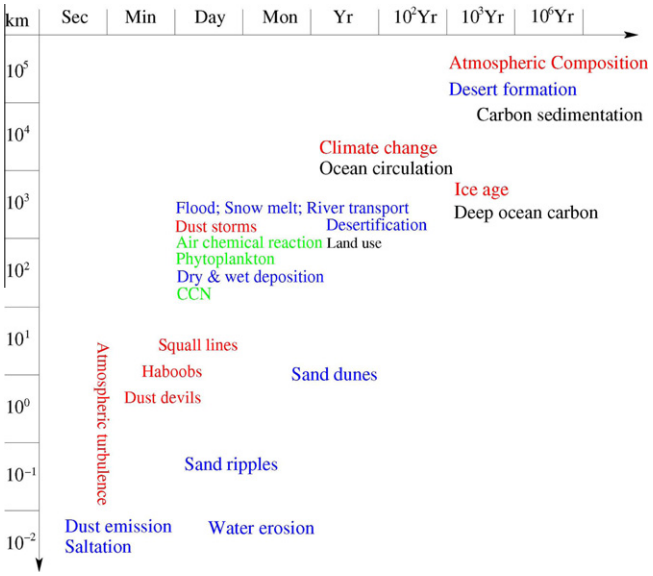

Fig. 3. Approximate spatial and temporal scales of the processes involved in the dust cycle.

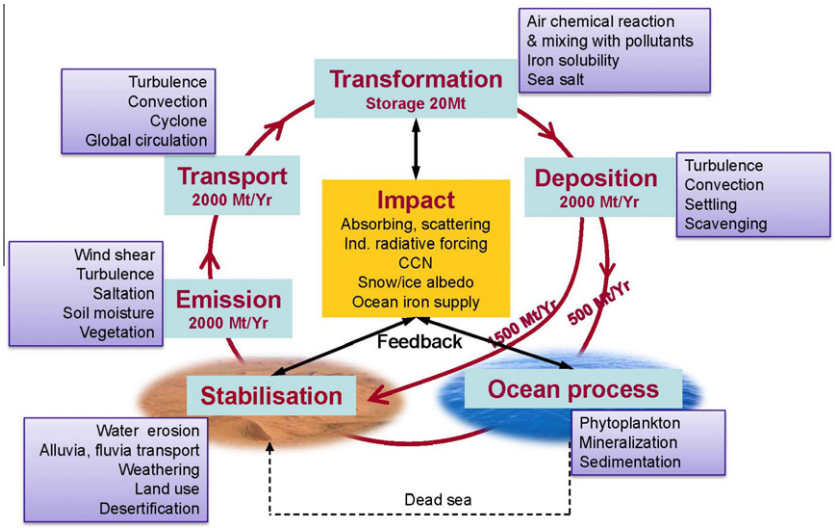

Fig. 2. An illustration of the dust cycle in the Earth system and the main processes in which dust plays an important role.

Table 4
Comparison of global and annual mean dust budget between several model studies.

	Emission (Tg yr^{-1})	Dry dep (Tg yr^{-1})	Wet dep (Tg yr^{-1})	Dry/Wet	Load (Tg)	Lifetime (days)	Size range (μm)
Takemura et al. (2000)	3321	2670	651	4.1	13.8	1.5	0.2–20
Ginoux et al. (2001)	1814	1606	235	6.83	35.9	7.2	0.2–12
Chin et al. (2002)	1650	1483	183	8.1	28.7	6.3	0.2–12
Tegen et al. (2002)	1100	724	374	1.94	22.2	7.4	0.2–44
Werner et al. (2002)	1060	811	244	3.32	8	2.8	0.2–44
Zender et al. (2003)	1490	866	607	1.43	17.4	4.3	0.1–10
Luo et al. (2003)	1654	823	798	1.03	23	5.1	0.1–10
Miller et al. (2004)	1019	595*	414*	1.44	14.6	5.2	0.2–16
Tanaka and Chiba (2006)	1877	1202	675	1.83	14.6	2.8	0.2–20

* Calculated from presented lifetime.

Table 5
A summary of three dust emission schemes.

Scheme	Reference	Expression	Comments
Scheme-I	GP88	$F = \alpha_g u_*^n (1 - u_{*_t}/u_*)$ $F(d_1) = p_{ad}(d_i)\Delta d_1 F$	Hypothesis; not spectral
Scheme-II	MB95	$F/Q = a_1 \exp(a_2 \eta_1 - a_3)$ $F(d_i) = p_{ad}(d_i)\Delta d_1 F$	Empirical, $a_1 = 100$, $a_2 = 0.31$, $a_3 = 13.82$; not spectral
Scheme-III	S04	$F(d_i; d_s) = c_y \eta_{fi}[(1-\gamma) + \gamma\sigma_p]$ $(1+\sigma_3)\frac{Q(d_s)g}{u_*^2}$ $F(d_i) = \int_{d1}^{d2} F(d_i; d_s) p_s(d)\delta d; F$ $= \sum_{i=1}^{1} F(d_i)$	Theory; spectral

GP88: Gillette and Passi (1988); MB95: Marticorena and Bergametti (1995); S04: Shao (2004).

and transport under favorable climatic and geomorphic conditions. At a regional scale the Lake Eyre and Murray-Darling Basins of Australia provide a good example (Bullard and McTainsh, 2003). These basins are covered with large areas of sedimentary deposits which are fed by internally-draining rivers. Rainfall in the humid upper catchments of the basins entrain soils and transport the fines to inland dust source regions, from which dust is entrained and wind-transported back over the upper catchments.

A full appreciation of time-scales relevant to the global dust cycle involves events extending: (i) over the Neogene ($\sim 10^7$ years) related to, for example, Tibetan Plateau formation and the formation of the Northeast Asian arid zones; (ii) the Quaternary, involving the changes at glacial-interglacial time scales ($\sim 10^5$ years) in sources and atmospheric loading and the formation of large areas of dust deposition; and (iii) Anthropocene (Crutzen and Stormer, 2000) involving changes provoked by the impact of people, with relevant time scales of up to 10^4 years (e.g., Ruddiman, 2007). Embedded within these time scales are also the shorter more abrupt climate events, such as Dansgaard–Oescher/Heinrich events which appear to have had a strong global aeolian signature (e.g. Porter and An, 1995).

As already noted, the dust cycle is closely related to the energy and carbon cycles. Dust emission is a highly selective process leading to an enrichment of organic matter in dust and to the redistribution of carbon during their transport (McTainsh and Strong, 2007). Dust transport is also associated with the supply of iron to the surface ocean, which limits ocean productivity in HNLC (High-Nitrate and Low Chlorophyll) oceans, and its exchange of CO_2 with the atmosphere (Fig. 2). Thus, dust acts as a powerful agent in the global carbon cycle (see Section 4). Dust as an aerosol scatters and absorbs radiation in the atmosphere and acts as CCN influencing the optical properties of clouds and their rain-making potential. There is also speculation that the Saharan dust affects the patterns of precipitation over the Atlantic and even the development of tropical cyclones. In addition, dust deposition substantially increases the albedo of snow/ice surfaces (see Section 3). Dust and surface water are also closely linked and the dust cycle is incomplete without water, as discussed earlier. The impacts of the dust cycle on other cycles also generate various feedbacks. On geological time scales, for example, extended periods (10^3 years) of increased dust flux are well correlated with glacial periods of low CO_2 (Maher et al., 2010; Martínez-Garcia et al., 2009). On synoptic time scales, the presence of dust increases the stability of the atmospheric boundary layer and reduces the global dust emission by as much as 15% (Perlwitz et al., 2001).

The past provides great insight into how the global dust cycle functioned over a range of spatial and time scales. The challenge is to understand how it may evolve in the future. From present climate projections it seems likely that there will be a significant reorganisation of the arid zone, according to the IPCC (Intergovernmental Panel on Climate Change) AR4 (Accessment Report 4) (IPCC, 2007), with some parts of the world such as southern Australia poised to experience a significant further downturn of precipitation over the next few decades. These changes in precipitation and unrealistic landuse practices can combine (and in the case of the northern 'wheatbelt' of Western Australia, already have) and create serious wind erosion problems. More globally, the role of dust aerosol needs to be more firmly established and incorporated into climate models for climate projections.An understanding of the issues both of the past and the future requires that the dust cycle is seen as an important element of the Earth system.

2.2. Dust sources

Our understanding of the present-day dust sources is largely based on the information derived from dust weather records (e.g. Kurosaki and Mikami, 2005), satellite and ground-based remote sensing (e.g. Prospero et al., 2002), dust monitoring networks (e.g. Holben et al., 2001) and numerical models (e.g. Tanaka and Chiba, 2006). Quantitative and 3-D dust observations with high-spatial and temporal resolutions are increasingly made through a combination of data from satellites, networks of lidars and radiometers, air-quality monitoring and weather stations. There has been a continuing effort to quantify the intensities of the dust sources (Table 1). The more recent estimates range from 1000 Mt yr^{-1} to 5000 Mt yr^{-1} converging to a value between 1000 and 2000 Mt yr^{-1}. This convergence is primarily due to the fact that two similar constraints are imposed on global dust models, namely, the global dust load which can be retrieved from satellite observations and the dust residence time in the atmosphere. All these estimates have large uncertainties which are yet to be quantified.

Dust activities are monitored through the network of weather stations distributed around the world. This is a powerful data set, because for some of the dust prone areas, dust weather observations have been continuous for more than 50 years. At weather stations, dust weather phenomena (e.g. dust in suspension, local blowing dust, dust storms and severe dust storms) together with visibility are reported at regular intervals (e.g. 3 h). Dust concentration can be estimated from visibility using empirical relationships and dust concentration maps can be compiled by spatial interpolation of dust concentration derived from visibility at individual weather stations (e.g. McTainsh, 1998). A dust weather climatology is now well established by analysis of synoptic dust weather records (McTainsh et al., 2005; Shao and Dong, 2006; Klose et al., 2010; O'Loingsigh et al., 2010). The disadvantage of dust weather data is the relatively sparse distribution of weather stations in key source areas, such as the central Sahara, the Gobi and Taklimakan Deserts and central Australia, and the low and often variable frequencies of observation times.

Sensors on board satellites detect the radiances of various types from the Earth to allow the monitoring of dust events, the potential to identify dust hot-spots, to derive land-surface parameters required for dust modelling and to derive dust-related quantities such as optical thickness, particle size, etc. TOMS (Total Ozone Mapping Spectrometer, 1983–2004 except May 1993-Jul 1996) and OMI (Ozone Monitoring Instrument, 2004) have long provided aerosol index for dust measure. Recently employed active remote-sensing technology has enhanced the capacity of satellites in dust quantification. CALIPSO/CALIOP (Cloud-Aerosol Lidar and Infrared Pathfinder Satellite Observations/Cloud-Aerosol LIdar with Orthogonal Polarization, 2006) measures aerosol extinction coefficient and Single-Scattering Albedo (SSA) to allow for the quantification of aerosol profile with a 30 m vertical resolution and 70 m horizontal resolution.

The TOMS data have been shown to be very useful for mapping the distribution of absorbing aerosols (mainly dust and black carbon) measured in terms of an aerosol index (AI). TOMS AI has been used to identify areas of high dust concentration, despite its known uncertainties in areas such as North East Asia. Using the TOMS data Prospero et al. (2002) identified two primary dust source regions in North Africa: the Bodele Depression; and an area in the western Sahara, comprising portions of Mauritania, Mali and southern Algeria. The secondary dust sources in North Africa include Tunisia and northeast Algeria; the Libyan Desert and Western Desert (Sahara El Gharbiya); the Nubian Desert and Northern Sudan; and the Horn of Africa and Djibouti.

A problem with using satellite data for dust source identification is that satellites observe transported, as well as, entrained dust. Klose et al. (2010) analysed dust weather data between the years 1983–2008 and identified the existence of a Sahel dust zone (SDZ). SDZ is active between December and April, and is most prominent in February and March and relatively weak between July and October (Fig. 4). The seasonal variation of SDZ is closely related to that of the monsoon trough. The zone of maximum dust activity is located to the north of, and evolves with, the monsoon trough, consistent with satellite observations (Engelstaedter and Washington, 2007). The relatively frequent dust activities south of the monsoon trough in summer are related to small-scale disturbances, such as dust devils, haboobs generated by cold air outflows from convective events, nocturnal low-level jets and easterly waves (Knippertz and Todd, 2010). The TOMS (for 1983–2004, excluding May 1993–Jul 1996) and the OMI (for 2005–2008) data not only confirm the results derived from the surface weather data, but also show that the dust zone stretches further over the Atlantic. There is however an AI maximum in the central western Sahara in summer that is not seen from the synoptic records. It is uncertain whether the AI maximum indeed represents high levels of dust concentration because the AI is sensitive to boundary layer height.

More recently, international research projects have been organised to identify the sources of African dust. For example, Bou Karam et al. (2008) presented a case study of the 7 July 2006 dust event within the framework of the African Monsoon Multidisciplinary Analysis (AMMA) project, in which they investigated dust mobilization and transport in the intertropical discontinuity region (ITD) in western Niger. The latter authors used lidar and dropsonde observations to analyse the structure of dust plumes. Dust in the monsoon flow was found to be mainly mobilized by the passage of a density current related to a mesoscale convective system and strong near-surface winds and turbulence. Knippertz et al. (2009) analysed the synoptic conditions for dust emission and transport in the northern Sahara during the Saharan Mineral Dust Experiment (SAMUM) in May and June 2006. Backward trajectory analyses at different atmospheric heights as well as synoptic analyses indicated the lowlands between Tunisia and central Algeria to be the main dust source during the days of investigation. The AMMA and SAMUM experiments have significantly improved our understanding of atmospheric systems which generate African dust.

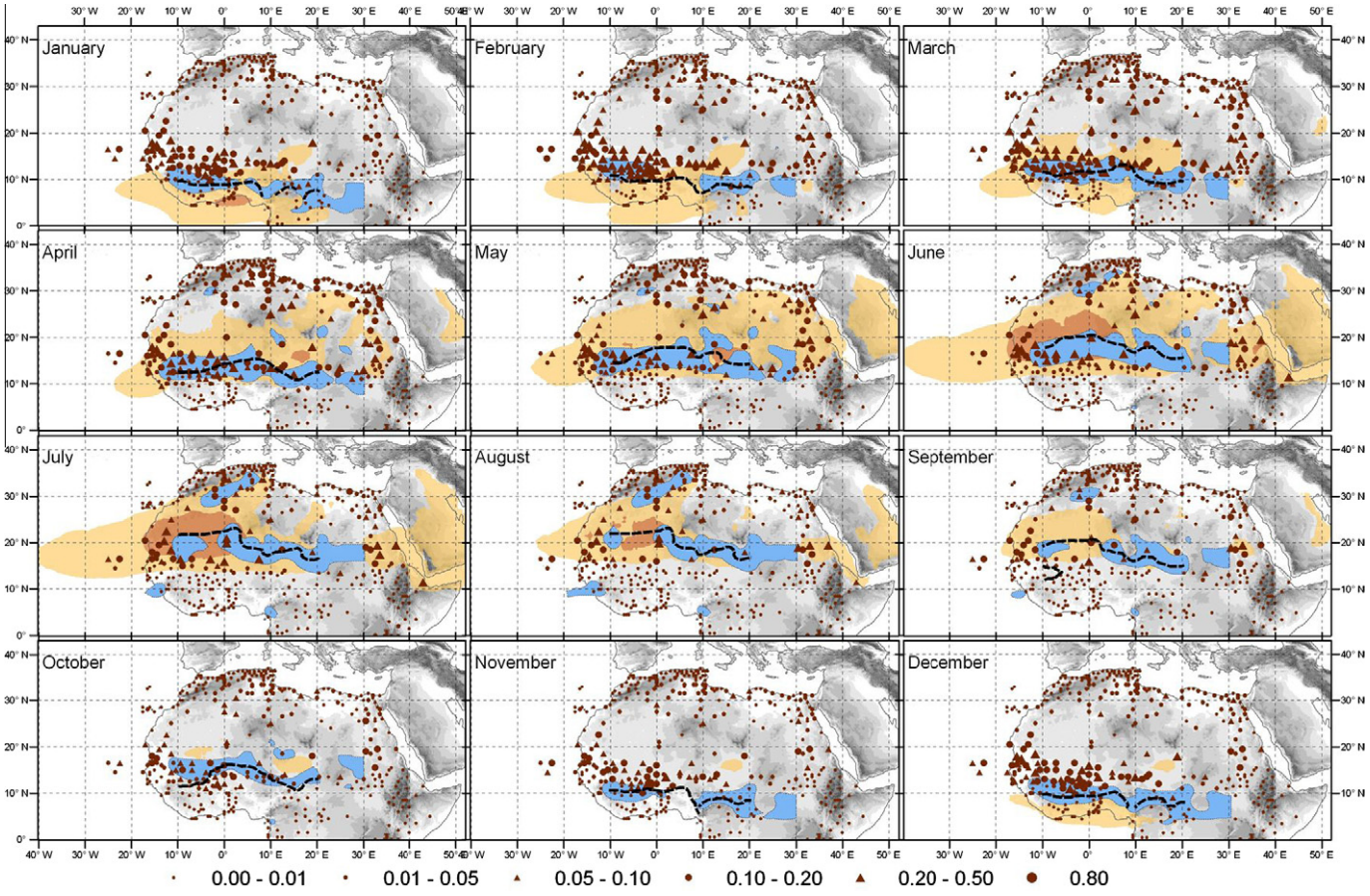

Fig. 4. Relative frequency of dust events over the 26 year period from 1983 to 2008 calculated separately for individual months. The topographic height is shaded in black. The blue areas represent the $8 \times 10^{-6}\,s^{-1}$ level of horizontal convergence and the black dashed lines the position of the lowest 925 hPa geopotential height between the Equator and 28°N (an indication of the ITD position) as derived by Lavaysse et al. (2009). Yellow and orange areas indicate regions of monthly averaged TOMS/OMI AI exceeding 1.8 and 3 (from Klose et al., 2010).

The second largest dust source on Earth includes the deserts in China and Mongolia. In winter, this region is dominated by the Siberian High and a fraction of the desert is frozen or covered by snow. The soil thaws in spring, leaving behind a loose surface prone to wind erosion. In March, April and May, the Gobi region is affected by Mongolian cyclones which are mainly responsible for severe Asian dust storms. The dust raised from the Gobi is transported south-eastward and the coarse fraction is deposited on the Chinese Loess Plateau. Strong westerly winds carry the dust thousands of kilometers over the Pacific Ocean along a corridor between 25°N to 45°N, influencing the eastern parts of China, Korea, Japan and the Pacific Ocean. It has been shown in numerous studies (e.g. Zhou, 2001) that the Tarim Basin has a very high frequency of dust events (maximum 47% at Hetian, 80°E, 37°N). Dust events over the Gobi are intense but somewhat less frequent (a maximum of 15%). Shao (2008) derived potential dust source regions by combining dust weather records, visibility data and topography, land-use and vegetation data (Fig. 5). Dust concentration is first estimated from visibility for individual weather stations as shown in Fig. 5a. The potential dust source region is then identified by excluding water, snow and vegetation surfaces (Fig. 5b) and finally the potential dust source regions are determined by taking topography into consideration (Fig. 5c).

Australia is the largest dust source in the Southern Hemisphere. Based on dust weather records for 1960–1984, McTainsh and Pitblado (1987) identified five regions with high dust storm frequencies in Australia: central Australia; central Queensland; the Mallee region; the Nullarbor Plain and coastal central western Australia. The highest frequencies were in central Australia and subsequent studies confirmed this general regionalization (McTainsh and Leys, 1993).

Wind erosion is most active in El Nino years when eastern Australia experiences reduced rainfall and decreased vegetation cover (e.g. 1993–1994 and 2002–2003 summer). The clearance of native vegetation for farming and grazing in semi-arid Australia in the past 200 years is thought to have contributed to stronger wind erosion in south-western Australia, the Eyre Peninsula and the Mallee Country of Victoria and New South Wales. In southern Australia, dust activity starts in September, peaks in February and weakens in May. In northern Australia, wind erosion occurs mostly during the spring to early summer.

Dust sources in other areas include

- Middle East: the Tigris-Euphrates alluvial plain in Iraq and Kuwait; the low-lying flat lands along the Persian Gulf and the Ad Dahna and the Rubal Khali deserts; the Oman coastal area between 54.0°E and 58.0°E to 200 km inland;

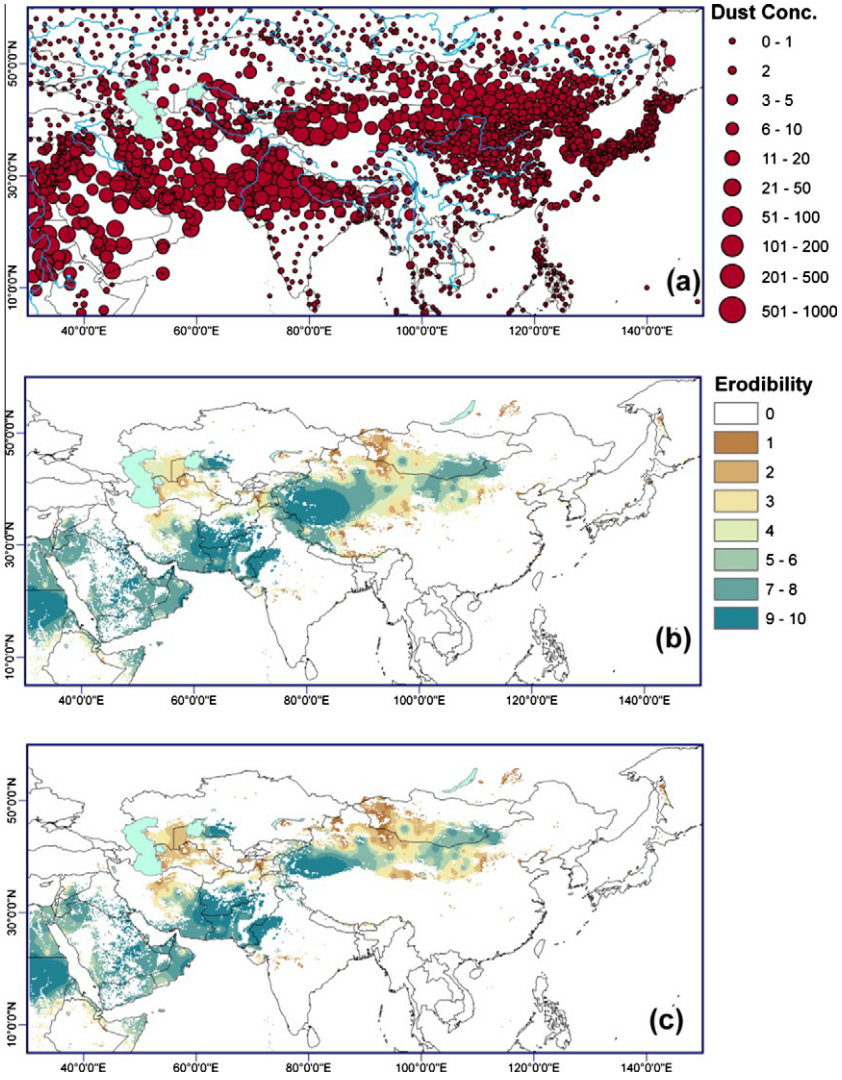

Fig. 5. Potential regions of dust sources, derived by combining visibility data and GIS topography, land use and vegetation data. (a) Dust concentration estimated from visibility data for individual weather stations; (b) Potential dust region after taking into consideration water, snow and vegetation surfaces; (c) Potential dust region after taking topography into consideration (from Shao, 2008).

- Central Asia: Kasakhstan to the northeast of the Aral Sea; sandy deserts between the Caspian and Aral Seas; the Turan Lowlands and southeast part of the Turan Plain;
- Southwest Asia: the Great Salt Desert in the basin to the south of the Reshteh-ye Kuhha-ye Alborz mountains; Seistan Basin and Registan bordering Iran, Afghanistan and Pakistan; Makran coastal area; Thar Desert together with the arid regions of the Indian Rajasthan Desert;
- Unites States: areas to the west and southwest of the Great Salt Lake, the Great Salt Lake Desert and the Bonneville Salt Flats; the Salton Trough of southernmost California and northern Mexico; south of the USA – Mexico border.

2.3. Dust sinks

Dust deposition measurements are relatively few and incomplete. Earlier deposition rate measurements on land (excluding mainland China) range from 3.5 g m^{-2} yr^{-1} in Japan, to 200 g m^{-2} yr^{-1} in the Niger (McTainsh, 1999), and in Asian desert areas, rates range between 14 and 2100 g m^{-2} yr^{-1} (Zhang et al., 1997). Dust deposition rates over the oceans are much lower; from less than 0.001 to more than 10 g m^{-2} yr^{-1} (Pye, 1984). Duce et al. (1991) provided a review of the atmospheric input of aerosols to the world oceans, using data obtained during cruises and measurements at a number of sites for the Atlantic, Pacific and Indian Oceans (Table 2). They estimated dry deposition from dust concentration and dry-deposition velocity and wet deposition from dust concentration and a precipitation-scavenging ratio. Table 2 shows that dry deposition rates are around half of wet deposition rates in most oceans (excluding the North Atlantic). There are two areas of maximum dust deposition (about 10 g m^{-2} yr^{-1}), one in the North Atlantic due to Saharan dust and one in the North Pacific due to Asian dust. Listed in Table 2 are the deposition estimates from several other studies – the degree of disagreement between the estimates is considerable.

Dust deposition estimates for a number of sites in China, over the East China Sea and in the Chinese desert regions can be found in Gao et al. (1997) and Zhang et al. (1997). The data from Gao et al. (1997), given in Table 3, show that areas close to source have much larger deposition rates than more distant areas. For example, the deposition rate in the Ulan Buh desert, China (670 g m^{-2} yr^{-1}) is nearly 70 times that over the North Pacific (10 g m^{-2} yr^{1}). Liu et al. (2004) measured monthly dust-deposition rates at Gaolan (Loess Plateau, Gansu, China) over the period May 1998 – April 2000 and found the annual average dust-deposition rate to be around 133 g m^{-2} yr^{-1}. The rate of dust deposition during individual dust storms, reaching 11,720 g m^{-2} yr^{-1}, can be many times the annual average rate. The scatter among model-estimated dust deposition is again quite large, as shown in Table 3. There are large discrepancies in all of the measurements listed in the table. These results suggest that our present quantitative understanding of the global dust cycle is still somewhat limited.

For selected dust events, more detailed dust budget data are available from regional scale dust models. For example, Shao et al. (2010) carried out a numerical simulation of the 1–10 March 2004 severe dust event in North Africa. Over the 10 day period, the total dust emission, dust deposition and net dust emission (for particle size $d < 32$ μm) were respectively 716 Mt, 608 Mt and 107.6 Mt. A net of 79.8 Mt dust was provided to the global atmosphere. The total dry deposition and total wet deposition to ocean were respectively 6.7 and 0.6 Mt, which is similar to the North Atlantic dust deposition results of Duce et al. (1991, Table 2).

2.4. Transport patterns

The global pattern of dust transport is depicted in Fig. 6. According to D'Almeida (1986), Saharan dust has four main trajectories: (i) southward transport over the Sahel and the Gulf of Guinea (60% of the Saharan dust emission, but <5% of the dust reaches 5°N); (ii) westward transport to the Atlantic (25% of emissions); (iii) the northward transport to Europe (10%); and (iv) the eastward transport to the Middle East (5%). More recent studies show a similar picture (Engelstaedter and Washington, 2007; Klose et al., 2010; Knippertz and Todd, 2010): Saharan dust is primarily transported towards the monsoon trough by northeasterly wind and then westward by the easterlies in the tropics. The southward and westward transport is thus due to the same synoptic systems as detailed in Klose et al. (2010). In winter, more dust is transported along the southerly route, while in summer it follows a more westerly route (Fig. 6).

The emission and transport of dust from the Middle East and the Indian Subcontinent are associated with the Indian monsoon trough. The monsoon low located over the subcontinent and the high located to the northeast of the Mediterranean can generate strong northerly winds which produce dust storms and transport dust towards the Indian Ocean.

In Northeast Asia, the motion of the Mongolian cyclones and the cold air generally follow the East Asian trough. Dust from the

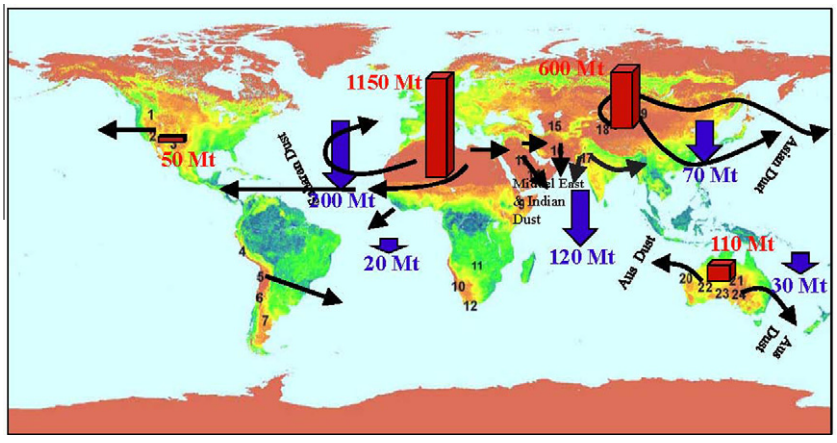

Fig. 6. Main routes of dust transport (arrows) and locations of the world's major deserts, including: (1) Great Basin, (2) Sonoran, (3) Chihuahua, (4) Peruvian, (5) Atacama, (6) Monte, (7) Patagonia, (8) Sahara, (9) Somali-Chabli, (10) Namib, (11) Kalahari, (12) Karroo, (13) Arabian, (14) Rub al Khali, (15) Turkestan, (16) Iranian, (17) Thar, (18) Taklimakan, (19) Gobi, (20) Great Sandy, (21) Simpson, (22) Gibson, (23) Great Victoria and (24) Sturt. The magnitudes of dust emission from different regions are given in Mt and indicated using bars and the depositions to the oceans are also given in Mt and indicated by thick arrows.

Taklimakan and the Gobi Desert is primarily transported toward the southeast and then the northeast. Sometimes, Asian dust can reach the west coast of Canada and the United States. There is a notable effect of dust source elevation upon dust transport (e.g. Kai et al., 2008). The Tarim Basin is no more than 1000 m above sea level, but is surrounded by mountains of c.a. 3000 m. The Taklimakan dust is first lifted vertically by convection and basin-scale mountain-valley circulation to 8–10 km above sea level. Due to the strong westerly flow in the upper atmosphere, the uplifted dust can travel more than once round the Earth (Uno et al., 2009). This implies that the residence time of the Taklimakan dust in the atmosphere can be more than two weeks, which is much higherthan the residence times of 4 ± 2 days reported in other studies (e.g. Textor et al., 2007). The elevation of the Gobi Desert is much lower and the Gobi dust transported by the cold air flows is confined to a shorter distance than the Taklimakan dust.

Australian dust is transported across the continent along two major routes: the south-east route which passes out over the southern Pacific Ocean and the north-west route which passes out over the Indian Ocean (McTainsh, 1989; Fig. 8). More recent event-based studies have shown that there is a wider range of trajectories within the south-east route than was first thought (McGowan et al., 2000; Shao et al., 2007; McGowan and Clark, 2008; Mackie et al., 2008).

3. The D-cycle and E-cycle

Dust and other aerosols, as well as clouds, water vapour and other greenhouse gases, affect transfers of solar and terrestrial radiation in the atmosphere. Anthropogenic aerosols cause a net global cooling effect which is believed to be comparable in magnitude to the warming effect due to anthropogenic greenhouse gases. However, as shown in the IPCC AR4 (IPCC, 2007), large uncertainties are associated with the radiative forcing of various types of greenhouse gases and aerosols and are of great concern in global climate studies. With this background, the research on mineral aerosol radiative forcing has been extremely active in recent years both in model simulation and observations using ground-based, aircraft and satellite-borne instruments (Huebert et al., 2003; Bush and Valero, 2003; Nakajima et al., 2003, 2007). The interference of dust in the energy cycle of the Earth system is not limited to radiation transfer in the atmosphere, because dust also affects snow/ice albedo and limits ocean productivity which in turn affects the atmosphere-ocean carbon exchange.

3.1. Direct radiative forcing

The impact of dust on atmospheric radiation transfer is often represented using the radiative forcing at the bottom of atmosphere (BOA) and at the top of atmosphere (TOA). The dust radiative forcing at BOA is known to be larger than that at TOA where the negative forcing (cooling) at visible-light wavelength is partially compensated by the positive forcing (warming) at thermal wavelengths. Particular attention has been paid to the effects of the Saharan and the Asian dust.

Tompkins et al. (2005) showed that a correction in the aerosol optical depth in the ECMWF (European Centre for Medium-Range Weather Forecasts) forecast model could remove the large bias related to the weakening and poleward migration of the African easterly jet in the 10-day forecast. Using the UK Met Office Unified Model, Haywood et al. (2005) found a 50 Wm^{-2} difference between the satellite and model TOA outgoing long-wave radiation over cloud free areas in the western Saharan heat low region. A plausible explanation for this discrepancy is the neglect of mineral dust in the model. Cavazos et al. (2009) conducted a detailed study on the 6–11 March 2006 Saharan dust event using the Regional Climate Model version 3 (RegCM3). This dust event was associated with a mid-latitude cold air outbreak over the northern Sahara. The anomalously strong northerly winds, which propagated from west to east over the Sahara during the study period, resulted in dust mobilization from multiple dust sources across the domain. For this event, Saharan dust had a profound impact on the surface solar radiation budget of $\sim -140\ Wm^{-2}\ \tau^{-1}$ (τ is unit atmospheric optic thickness). The shortwave radiative effect at TOA was about $-10\ Wm^{-2}\ \tau^{-1}$ over this study domain. The dust radiative effect caused an anomaly of 2-m air temperature between −10 and +4 K.

Such strong radiative forcing is expected to generate negative feedbacks. Perlwitz et al. (2001) suggested that dust radiative forcing could reduce the global dust emission by up to 15%. The negative feedback is thought to occur through the modification of the planetary boundary layer: reduced incident radiation by the dust layer leads to reduced downward momentum flux and hence, reduced dust emission. Heinold et al. (2008) studied the feedbacks between dust and the boundary layer using a regional dust model and found that the feedbacks contribute to the formation and breakdown of the low-level jet in the Bodélé Depression.

The magnitude of radiative forcing of Asian dust is comparable to that of the Saharan dust. Based on the ACE-Asia data, Seinfeld et al. (2004) estimated that dust radiative forcing at TOA and BOA was respectively −5.5 and −9.3 Wm^{-2} for the area (20°–50°N, 100°–150°E) during 5–15 April 2001. The radiative forcing of Asian dust was monitored at Gosan, Korea, a site that is heavily impacted by Asian aerosols. MODIS (Moderate Resolution Imaging Spectroradiometer) and AERONET (Aerosol Robotic Network) Sun/sky radiometer measurements showed significant seasonal and geographical variations in aerosol optical depth (AOD), with large AODs over the industrialized east coastal regions of China in spring and summer. At Gosan, the monthly mean AOD at 675 nm ranged between 0.12 and 0.36. Large AODs were observed from April to June (~0.33), with low-to-moderate AODs in the other months. The SSA exhibited relatively low values from February to May (<0.93), indicating the presence of light-absorbing aerosols, but high values (>0.93) in the other months. Based on 3-year AERONET measurements (Yoon et al., 2005), the mean aerosol forcing efficiency at 670 nm at Gosan during the spring dust season was evaluated to be $-80.57 \pm 13.2\ W\ m^{-2}\ \tau^{-1}$ at BOA and $-29.97 \pm 4.9\ W\ m^{-2}\ \tau^{-1}$ at TOA. These findings are consistent with the more recent results of Kim et al. (2010) who found that the annual average clear-sky direct forcing at BOA was $-27.55 \pm 9.21\ W\ m^{-2}$ ($-91.85 \pm 11.12\ Wm^{-2}\ \tau^{-1}$), and $-15.79 \pm 4.44\ W\ m^{-2}$ ($-53.76 \pm 6.70\ W\ m^{-2}\ \tau^{-1}$) at TOA, thereby leading to an atmospheric absorption of $11.76 \pm 5.82\ W\ m^{-2}$. From March to June, the aerosol radiative forcing at BOA ranged between −27.29 and $-34.76\ W\ m^{-2}$ (-85.33 and $-97.19\ W\ m^{-2}\ \tau^{-1}$), whereas at TOA between −16.84 and $-19.10\ W\ m^{-2}$ (-51.82 and $-56.05\ W\ m^{-2}\ \tau^{-1}$), and the atmospheric forcing ranged between 10.45 and 16.41 $W\ m^{-2}$. The atmospheric absorption caused an increase in atmospheric heating of 1.5–3.0 K day^{-1}. The strongest radiative heating was observed from April to May (>2.5 K day^{-1}).

Huang et al. (2009) studied dust radiative forcing over the Taklimakan desert. Under light, moderate and heavy dust conditions, the dust heating effect was up to 1, 2 and 3 K day^{-1}, respectively. For a strong dust event, the maximum daily mean radiative heating rate reached 5.5 K day^{-1} at 5 km, and the averaged daily mean dust radiative forcing were $-41.9\ W\ m^{-2}$ at BOA and $44.4\ W\ m^{-2}$ at TOA, thereby an atmospheric absorption of $86.3\ W\ m^{-2}$. About two thirds of the radiative forcing at TOA was due to longwave radiation, while about 90% of the atmospheric warming was due to solar radiation. At BOA, about one third of the dust cooling effect was compensated by its longwave warming effect. The modifications of radiative energy budget by dust over

the Taklimakan are expected to have major implications for the regional climate of the Tarim Basin.

3.2. Dust and clouds

About 60% of the Earth's surface is covered with clouds. On a global average, clouds cool the Earth system at the TOA. Measurements from the Earth Radiation Budget Experiment (ERBE) (Collins et al., 1994) indicate that small changes to cloud macro-physical (coverage, structure, altitude) and microphysical properties (droplet size, phases of water) have significant effects on climate. For instance, a 5% increase in shortwave cloud forcing would compensate for the increase in greenhouse gases that occurred during the period 1750–2000 (Ramaswamy et al., 2001). To study the dust effect on clouds, the dusty cloud properties were analyzed over northwestern China using MODIS and CERES (Clouds and the Earth's Radiant Energy System) data (Huang et al., 2006 a–c). On average, ice cloud effective particle diameter, optical depth and ice water path of cirrus clouds in a dust-loaded atmosphere are 11%, 32.8% and 42%, respectively, less than those derived from ice clouds in a dust-free atmosphere. Due to changes in cloud microphysics, the instantaneous net radiative forcing increased from $-161.6\ W\ m^{-2}$ for dust-free clouds to $-118.6\ W\ m^{-2}$ for dust-contaminated clouds (Huang et al., 2006b). The water path of dust-contaminated clouds is considerably smaller than that of dust-free clouds. The mean ice water path and liquid water path of dusty clouds are less than their dust-free counterparts by 23.7% and 49.8%, respectively. The long-term statistical relationship derived from the International Satellite Cloud Climatology Project (ISCCP) also confirmed that there is a significant negative correlation between a dust storm index and the ISCCP cloud water path. These results suggest that dust aerosols warm clouds, increase the evaporation of cloud droplets and reduce cloud water path the so-called semi-direct effect.

The semi-direct effect may play a role in cloud development over arid and semi-arid areas of East Asia and contribute to the reduction of precipitation (Huang et al., 2006c). Su et al. (2008) estimated the contribution to the cloud radiative forcing by dust direct, indirect and semi-direct effects using combined satellite observation and Fu-Liou model simulation. The four-year mean value of the combination of the indirect and semi-direct shortwave radiative forcing was $82.2\ W\ m^{-2}$, 78.4% of the total dust effect. The direct effect was only $22.7\ W\ m^{-2}$, 21.6% of the total effect. Because both primary and secondary indirect processes enhance the cloud cooling effect, the dusty cloud warming effect is mainly contributed by the semi-direct effect of dust aerosol. Using a two-dimensional spectral resolving cloud model, Yin and Chen (2007) simulated the effects of dust on the development of cloud microphysics and precipitation over northern China. Dust aerosols can act as CCN and IN (ice nuclei), i.e., the particulates around which cloud droplets form. CCN and IN may be either emitted directly or grown from primary particles of smaller sizes. The latter authors found that when dust particles are involved in cloud development as CCN and IN at the same time, the heating effect of dust aerosols and the increased dust aerosol loading suppress precipitation. This combined effect is due to the enhancement of CCN and is nearly overwhelmed by the stronger suppressing effect of IN (Chen et al., 2007). Furthermore, Han et al. (2008) found that the role of precipitation in suppressing dust storm occurrence is unimportant and that dust aerosols may play a more important role in suppressing the precipitation over arid and desert regions. This, in turn, could reduce the probability of precipitation, resulting in more complex and uncertain indirect effects. Due to the large spatial and temporal extent of desert dust in the atmosphere, the interactions of desert dust with clouds and land surfaces can have substantial climatic impacts.

Uncontaminated dust is assumed to be hydrophobic. Below-cloud scavenging is the dominant wet deposition process over in-cloud scavenging. As more hydroscopic compounds such as sulphates aggregate on their surfaces dust particles undergo transformations during transport (Levin et al., 2005). These coatings allow dust to act more efficiently as CCN (Andreae and Rosenfeld, 2008). In-cloud processes, especially for dust, remain poorly understood, and their representation in models is still rather crude. In most models, dust is treated as being fully hydrophobic and in-cloud scavenging is neglected (Shao et al., 2003), or fully hydroscopic as sulphate aerosols (Grini et al., 2005). In any case, the particle size dependency of in-cloud scavenging is not considered in dust models.

3.3. Dust as an air pollutant

A better quantification of dust optical properties remains a key challenge for reducing the uncertainties in climate simulations (Dubovik et al., 2002; Lafon et al., 2004). Aerosol optical properties depend on the physical and chemical characteristics of the particles and the state of mixing. For instance, the extinction efficiency for visible light depends strongly on particle size in the submicron range and SSA decreases with particle size. Dust particles vary in composition and the differences in dust mineralogy can drastically affect the magnitude of the aerosol radiative forcing in the infrared and the visible range (Sokolik et al., 1998; Quijano et al., 2000).

There are large variations in the dust refractive index. The imaginary part of this index, n_I, recommended by the WMO (World Meteorological Organisation) in 1983 was 0.008. For the Saharan dust, n_I is now estimated to be in the range of 0.0054–0.0066 at 360 nm and about 0.0025 at 440 nm (Dubovik et al., 2002). For Asian dust, Aoki et al. (2005) found a n_I of 0.0047 at 450 nm. One of the fundamental optical parameters is SSA. A slight change in SSA can result in a change of aerosol radiative forcing from negative to positive. For example, Won et al. (2004) showed that a 5% uncertainty in SSA resulted in 10–15% uncertainties in the aerosol direct radiative forcing. The SSA value recommended by the WMO (1983) was 0.63 at 500 nm, but the recent estimate is 0.97 at 640 nm for Saharan dust (Kaufman et al., 2001) and 0.98 at 500 nm for Asian dust (Seinfeld et al., 2004). Compared with pure dust aerosols, a smaller SSA value (0.906 at 670 nm) was observed downwind of the Asian continent when Asian dust and anthropogenic pollutants are mixed (Won et al., 2004).

3.3.1. Elemental composition and mineralogy

Dust particle shape, elemental composition and mineralogy strongly affect the optical characteristics of dust particles. Of particular importance is the presence of light-absorbing substances, such as iron-oxides (Dubovik et al., 2002; Lafon et al., 2004). Various water-soluble cations (Na^+, K^+, Ca_2^+, Mg_2^+) are well correlated with elemental indicators of dust and distinct differences exist between the Ca/Al, Si/Ca, and Fe/Ca ratios in Asian dust versus African dust. Information on the radiative properties of different dust minerals is even more limited than for elements, largely because of laboratory analysis constraints. QEMSCAN (Quantitative Evaluation of Minerals by SCANning electron microscopy), a new technology for automated mineral analysis of earth materials, including dusts and soils, offers exciting possibilities (Pudmenzky et al., 2006; Haberlah et al., 2010).

3.3.2. Mixing

The mixing state of the aerosols, i.e. whether they are internally mixed (aerosols individually comprising mixtures of different components), or externally mixed (mixtures of aerosols, each comprising a different single component) is important to the estimates of aerosol radiative forcing. For example, the internal mixing of

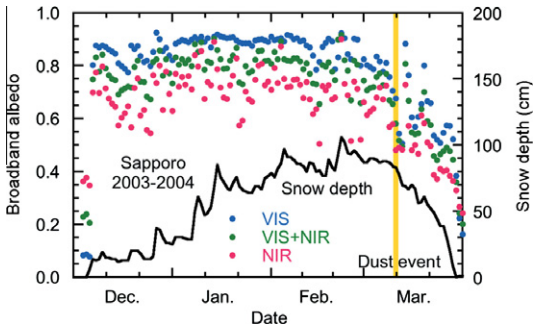

Fig. 7. Visible (VIS), shortwave (VIS+NIR), and near infrared (NIR) albedos averaged from 1131 to 1200 LT and snow depth at 1200 LT during the winter of 2003/2004 in Sapporo, Japan (from Aoki et al., 2006).

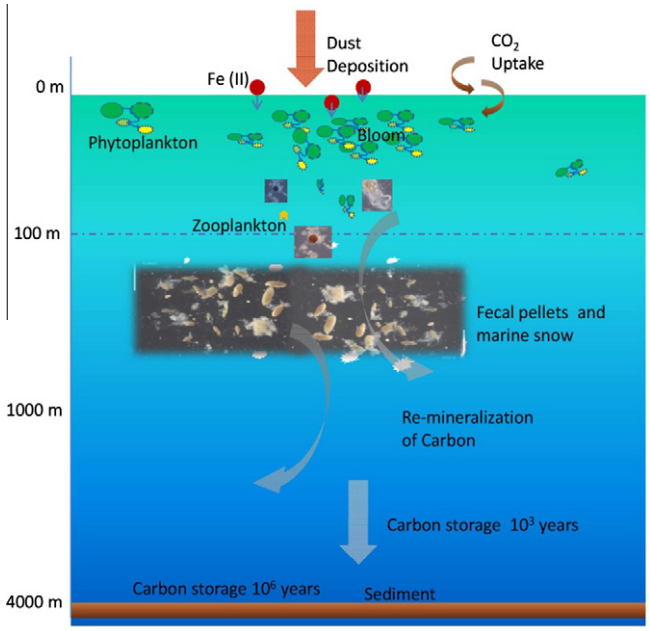

Fig. 8. Biological pump. The deeper the carbon sinks, the longer it will be removed from the atmosphere.

organic carbon with sulphate and dust can result in a net difference in radiative forcing of more than 1 W m^{-2} relative to the externally mixed case (Seinfeld et al., 2004). Dust and black carbon form aggregates, making dust more absorbing of visible and infrared light. When dust and anthropogenic substances interact, not only are their optical properties modified, but also their atmospheric lifetimes. Dust particles also mix with sea salt as they are transported in the marine boundary layer. This process increases dust particle size and enhances dust deposition to oceans by about 15% (Zhang, 2008).

3.3.3. Chemical Reactions with Air Pollutants

In some parts of the world (e.g. southern Europe, northeast Asia and southwest Asia), light-absorbing pollutants Pb, NO_{3-} and S_4O_{2-} are added to dust clouds during their transport. SO_2 oxidation, mainly originating from petrochemical activities, gives rise to the formation of H_2SO_4 (gas or particulate). This compound may form particulate $(NH_4)_2SO_4$ or NH_4HSO_4 in the presence of NH_3. This compound (gas), emitted through fuel combustion, may react with available HNO_3 formed after NO_x oxidation forming fine particulate NH_4NO_3. The stability of these salts depends on temperature, humidity and pH. Interaction of anthropogenic pollutants with mineral dust leads to secondary coarse $NaNO_3$ and $CaSO_4$ with minor amounts of $Ca(NO_3)_2$ and Na_2SO_4 (Gangoiti et al., 2006). Observations show that dust particles are often coated with sulphates by taking up sulphate precursor gases. Such chemical reactions are currently not well understood. Arimoto et al. (2006) showed that single dust particles typically do not contain large amounts of both sulphate and nitrate (or both sulphate and chloride), but rather one species to the exclusion of the other. It appears that the processes for production of these substances are competitive in nature. The consequent mixture or chemical products have very different optical properties compared to those of individual identities.

3.4. Dust and snow/ice surface albedo

The snow/ice-albedo feedback has long been recognized as a key process that affects climate (Budyko, 1969; Sellers, 1969). The IPCC climate models have consistently projected a major loss in sea ice cover by the mid 21st century, intrinsically related to the albedo feedback from reduced snow/ice cover (Chapin et al., 2005). The observations of Aoki et al. (2006) demonstrated the effect of dust deposition on the change of albedo. Figure 7 shows the dust fall on 11–12 March 2004 which resulted in a 100 times increase of snow impurity in the top 2 cm snow layer and halved the snow surface albedo. There is ample evidence that aerosols affect the energy and mass balance of snow and ice at all scales of time and space (Wagenbach et al., 1996; Delmonte et al., 2005; Clarke and Noone, 2007).

4. The D-cycle and C-cycle

A major dust research emphasis is to better understand the impact of dust deposition on ocean biomass productivity and the associated atmosphere-ocean carbon exchange (e.g. Maher et al., 2010). This is because the deep ocean contains nearly 85% of mobile carbon on the Earth and ocean phytoplankton is responsible for nearly half the annual CO_2 exchange and a majority of all carbon sequestered over geologic time. The formation of the deep ocean carbon reservoir is primarily due to the "biological pump" (Fig. 8). This process begins at the surface where phytoplankton converts CO_2 and other nutrients to biomass. Phytoplankton can then be consumed by zooplankton or die. Some dead phytoplankton and fecal pellets from the zooplankton, aggregate, and sink into the deep ocean. Other material decomposes as it sinks and releases carbon to deep-ocean waters where it can be stored for thousands of years. Some of the material sinks further to the ocean floor where it accumulates as sediment, and the associated carbon can be stored there for millions of years. The net result is a continual movement of carbon from the atmosphere to the deep ocean.

Martin and Fitzwater (1988) proposed the so called "Iron Hypothesis", i.e. that CO_2 reduction in the atmosphere during glacial maxima measured in ice-core samples may be related to increased iron supply from enhanced dust deposition to the ocean. Ice core records worldwide (Fig. 9) show that extended periods (10^3 years) of increased dust flux and enhanced iron delivery occurred several times over the past million years and these periods were well correlated with glacial periods of low CO_2 (Maher et al., 2010; Martínez-Garcia et al., 2009).

Satellite images and sediment trap flux observations show high correlation between regional ocean biological productivity (chlorophyll bloom) in the Arabian Sea and Indian dust storms (Kayetha et al., 2008). Ramos et al. (2008) suggested that diazotrophic cyanobacteria bloom (Fig. 10) in the NW African upwelling region may be related to Saharan dust storms and Yuan and Zhang (2006) reported that pinnate diatoms in North Pacific Ocean are

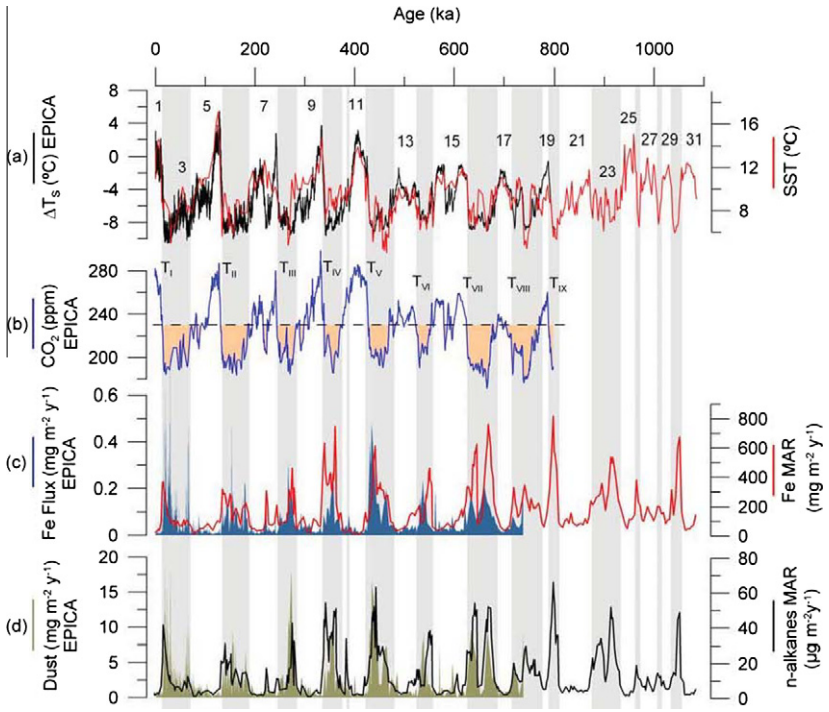

Fig. 9. FigMarine and terrestrial records over the past 1.1 Ma reconstructed from EPICA ice cores and alkenone data at Site PS2489-2/ODP1090. (a) Temperature from EPICA ice cores (black, Aarctica) and SST from PS2489-2/ODP1090 (red); (b) EPICA CO_2 concentrations. Filled are illustrates CO_2 concentration below 230 ppmv. (c) EPICA Fe flux (blue) and PS2489-2/ODP1090 Fe flux (red). (d) EPICA insoluble dust (light brown) and PS2489-2/ODP1090 C_{23-33} mass accumulation rate (blue). The highest levels of iron (gray vertical bands) correspond to the highest dust concentration, lowest temperature and CO_2 levels in every glacial cycle (for details see Martínez-Garcia et al., 2009).

Fig. 10. Bloom of Trichodesmium – Canary Islands, August 2004, may be associated with Saharan dust storms in July 2004 (Ramos et al., 2008).

related to Northeast Asian dust storms. A large body of oceanographic research and the geologic record support the notion that the availability of iron limits the growth of phytoplankton in large (but not all) areas of the ocean.

Recent modeling studies also support the biological pump hypothesis. Marinov et al. (2008) compared the effectiveness of three oceanic carbon capture mechanisms: (i) the biological pump; (ii) the calcium carbonate pump and (iii) the solubility pump. The calcium carbonate pump refers to the process that atmospheric CO_2 dissolved in ocean water leads to the formation of carbonate which combines with dissolved calcium to precipitate solid calcium carbonate ($CaCO_3$) to the ocean floor, while the solubility pump is a physico-chemical process that transports carbon as dissolved inorganic carbon from the ocean's surface to its interior. The latter authors concluded that the biological pump accounted for the majority of atmospheric CO_2 drawdown on millennial time scales. Schmittner and Galbraith (2008) suggested that the Southern Ocean is the primary region responsible for the large scale changes in atmospheric CO_2 and that changes in ocean circulation also play a role in determining the strength of the biological pump. The dominance of the Southern Ocean in large scale atmospheric CO_2 change is arguable, because the Southern Hemisphere does not have major continental dust sources. However, the details of this story are however yet to emerge (Mackie et al., 2008).

The principal source of iron to the surface ocean is aeolian dust (Jickells et al., 2005). The order of magnitude of dust deposition, as described in Section 2, is probably reasonable. There remains a need to quantify the deposition of iron associated with dust deposition. This requires the knowledge of iron content of dust source soils, and the chemical reactions that occur during dust transport (Mackie et al., 2008). While the iron content of the Earth's crust is on average 3.5% (Taylor and McLennan, 1985), it varies widely from region to region and also depends on particle size. For example, the iron content of Australian soils is 50% higher than the global average (Hand et al., 2004) and although iron-rich dust emission has been described in Australia (Bullard et al., 2007), global emission of iron-rich dust remains poorly quantified.

The dust-iron issue is rather complex because phytoplankton growth requires soluble iron (Fe^{2+}). Fe^{2+} in soils represents about 0.5% of total iron (Hand et al., 2004). However, measurements of Fe^{2+} in aerosols indicate a much higher solubility (Zhuang et al., 1992) implying that atmospheric chemical processes contribute to increased iron solubility during dust transport. A number of photochemical and cloud processes have been suggested (Jickells and Spokes, 2001), but the results to date are still uncertain. Fe^{3+} is soluble in acid solutions within clouds (Mackie et al., 2005) and under certain conditions Fe^{3+} can reduce to Fe^{2+}. Also, Meskhidze et al. (2008) reported that air pollution in Asia increases the iron solubility of Asian dust.

The dust cycle is thus a major component in climate research because of the dust–iron–CO_2 feedback. However, as Mackie et al. (2008) point out there remain many gaps in our knowledge of the inter-relationships between the dust cycle and the iron

cycle. The limiting role of iron in the productivity of oceanic waters also depends on whether oceanic waters are low-nitrate and low-chlorophyll (LNLC) or HNLC. There are also marked distinctions between Southern and Northern Hemisphere iron/dust biochemistry which require more detailed study.

5. Dust as a climate archive

The drawdown of atmospheric CO_2 due to possible dust-iron seeding during glacial stages draws attention to the important role that dust plays in long-term climate events. The stratigraphic record of dust deposition serves as an important palaeoenvironmental indicator of: (i) the climate of dust source and deposition areas; (ii) large scale-circulation/transport patterns and changes; and (iii) global-scale controls imposed on the climate system by dust loading – an important consideration in ocean-atmosphere general circulation model reconstructions of past climate states.

It is now recognized that atmospheric dust loads have varied significantly over orbital time scales (Kohfeld and Harrison, 2001; Maher and Kohfeld, 2009; Maher et al., 2010; Rea, 1994; Rea et al., 1998). Variations in dust loading are evident from stratigraphic archives provided by ice cores (Lambert et al., 2008), the deep sea record (Winckler et al., 2008) and terrestrial dust (loess) sequences (Ding et al., 2001). A most striking feature of these records is the pronounced variation of dust concentration over glacial/interglacial stages, with especially strong atmospheric loading evident during the Last Glacial Maximum (LGM) – c. 22,000 years ago – a claim also evident in model studies (Maher et al., 2010; Mahowald et al., 1999, 2006; Reader et al., 1999). These findings suggest that high latitude dust fluxes may have amounted to as much as 25 times their present value (Lambert et al., 2008), while in low latitudes this was considerably lower, though still >2.5 times present loads (Winckler et al., 2008) – a figure that has also been proposed to characterise the entire atmosphere (Mahowald et al., 1999). Maher et al. (2010) provided a very comprehensive synthesis of LGM dust loading estimates and reinforce the claims of elevated levels of dust fluxes identified in other studies.

5.1. Leoss records

Of the global terrestrial dust-loess records, the archives provided by the Chinese loess deposits are the most striking. The Chinese Loess Plateau covers an area of approximately 440,000 km^2, and with thicknesses in excess of 200 m, offers the most important terrestrial dust archive (Liu, 1965, 1985; Pye, 1984; Derbyshire, 2003). While the palaeoclimate significance of these deposits has been recognized for a long time in the European literature (since Von Richthofen, 1877, 1882), it was only with the development of appropriate dating techniques, that the potential of loess as a palaeoclimate indicator was fully realized (Heller and Liu, 1982; Lu et al., 1987, 1988). It is now apparent that the Chinese loess record provides a palaeo-environmental history that extends back as far as 22 Ma (Guo et al., 2002; Hao and Guo, 2007). The early part of the record provides insights into the timing of drying trends over East Asia associated with the retreat of the Paratethys and the uplift of the Tibetan Plateau (Guo et al., 2002). For the last few million years the Chinese loess stratigraphy provides a register of global Quaternary-style climate changes – indicating cold, dry glacials/stadials, with high rates of deposition, and more summer monsoon dominated interstadial/interglacial conditions – represented by palaeosols, indicating low rates of deposition (An, 2000). The high aerosol loading over China during glacial/stadial stages is likely to have had a direct effect on regional climates (Qin et al., 2009). Using magnetostratigraphy, an age structure of the Chinese loess has been developed, that has been correlated with the deep-sea oxygen isotope record, placing depositional events into the context of Milankovitch-scale climate variations (Kukla, 1987; Ding et al., 1994; Liu et al., 1999). However, the development of more reliable optically stimulated luminescence (OSL) dates suggests that some of the early claims may require revision (Lu et al., 2007). Similarly, claims that short-lived palaeoclimate events (the so called Heinrich events – see e.g. Cronin, 2009) can also be distinguished in the Chinese loess stratigraphy (Porter and An, 1995), have been challenged (Stevens et al., 2006). However, this challenge may have been premature, as Sun et al. (2010) recently showed, that with high sedimentation rates and weak pedogenesis, high-resolution grain size oscillations appear to record millennial scale climate events (Fig. 11).

Dust is an integral part of deep ocean sediments and the dust component of cores has been widely used to provide indications of the climate of source regions and the nature and intensity of the atmospheric circulation (Rea, 1994). The record from the Pacific has received a great deal of attention (Hovan et al., 1989; Rea, 1994; Rea et al., 1998; Pettke et al., 2002; Hyeong et al., 2005), complementing the Chinese loess record as an indicator of East Asian source area changes – both in terms of the onset and intensity of aridity and Tibetan Plateau uplift history, as well as giving indications of changes in the position of the Intertropical Convergence Zone during the Neogene (Hyeong et al., 2005).

5.2. Deep sea record

Over glacial-interglacial time scales, the deep sea dust record indicates that increased dust loading was a feature of glacial stages (Rea, 1994; Mahowald et al., 1999; Winckler et al., 2008). Moreno et al. (2002) suggested that the aeolian record of the western Mediterranean provides evidence of millennial scale Dansgaard–Oescher (D–O) events, with higher dust transport from the Sahara during cold stadial periods of the D–O cycles. The ocean record has proven to be a useful prompt in considering possible atmospheric circulation changes. Jilbert et al. (2010) showed that laminated sediments from the eastern Mediterranean contain Saharan dust which, over historical time scales, indicate the strength of the Westerlies over the Mediterranean region. Similarly, changes in the position of the Southern Hemisphere Westerlies in the Australian region have been proposed on the basis of the dust record of cores recovered from the Tasman Sea (Thiede, 1979; Hesse, 1994; Kawahata, 2002). Other Tasman Sea cores have proven useful in tracing the Neogene history of 'aridification' of Australia (Stein and Robert, 1986) and have been used to infer past dust transport and deposition processes (Hesse and McTainsh, 1999).

5.3. Ice cores

Ice cores have proven to be among the most informative registers of global palaeoclimate events since their potential was first recognized (Dansgaard et al., 1969, 1982). The available records (see summaries in Bradley, 1999; Cronin, 2009) provide very comprehensive insights into the global climate system, capturing both long term trends and millennial-scale changes (D–O events). Dust is an integral part of the ice core record and is prominent in cores both from Greenland and the Antarctic (Fischer et al., 2007), as well as being well represented in some low and –mid latitude cores (Thompson et al., 1997). Both the Antarctic and Greenland ice cores support dust model claims of higher dust loading during glacial stages. Using the $^{81}Sr/^{86}Sr$ and $^{143}Nd/^{144}Nd$ ratios of dust recovered from East Antarctic cores (Delmonte et al., 2010) and model studies (Lunt and Valdes, 2001), it has proven possible to identify Patagonia as being the main source for glacial stage dust, while other Southern Hemisphere sources (Gabrielli et al., 2010) are likely to

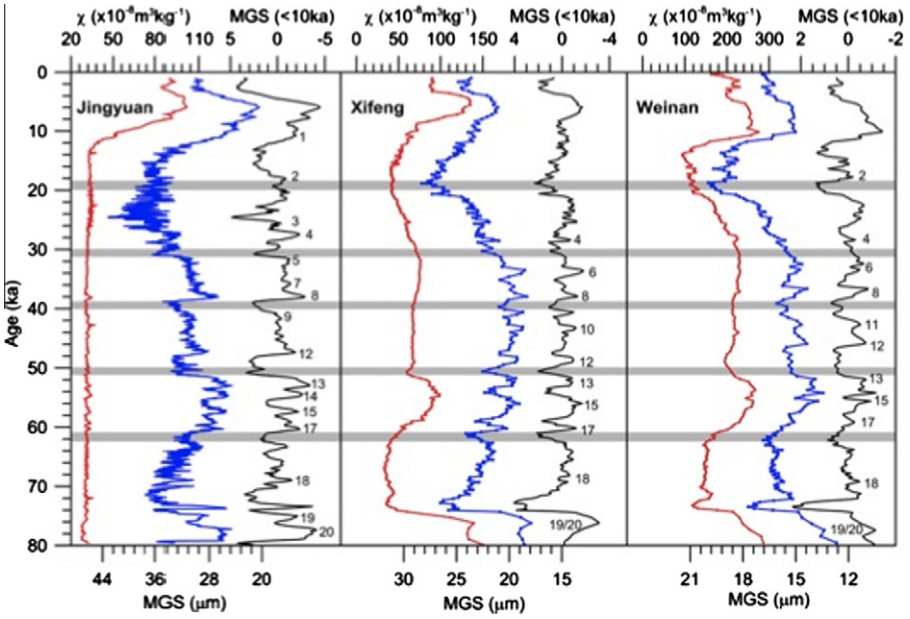

Fig. 11. High resolution grain size variations indicative of monsoon events: magnetic susceptibility (χ), mean grain size (MGS) and high-frequency (<10 kyr) component of the MSG record for three loess section. Grey bars indicate that coarsening of the MGS can be correlated between the three sections (Sun et al., 2010).

have been accessed during interglacials. The difference in sources between glacial and interglacial states relates to the readily available glacial stage dust sources presented by glacial outwash plains in Patagonia (Sugden et al., 2009).

The Greenland ice cores are of special significance with respect to the recognition of millennial-scale changes (Fuhrer et al., 1999; Stuiver and Grootes, 2000). During millennial-scale D–O events, dust concentrations were significantly smaller than during colder stadials (Fuhrer et al., 1999). Given the short-time scales over which D–O events occur (500–2500 years), and the abrupt changes in dust concentrations within these time periods, it seems more likely that the concentration changes reflect atmospheric circulation changes, with significantly higher wind speeds in the source areas (Fuhrer et al., 1999). Similarly, given the abrupt changes in dust concentration at the end of the Younger Dryas (about 11,000 years ago), it seems unlikely that they reflect environmental changes in the source areas (Alley et al., 1993). With the removal of the dust flux spike associated with D–O oscillations from the Greenland Ice Sheet Project 2 (GIPS2) record, the residual dust record is claimed to match Antarctic palaeoclimate events with a lag of several hundred years (Barker and Knorr, 2007). The authors argue that the variability reflects changes in the climate and aeolian surface conditions of East Asia, which is the source area for Greenland dust (Biscaye et al., 1997; Svensson et al., 2000).

All three dust archives have added greatly to our understanding of the climate system and global environmental events over a range of time scales. The ice core dust record represents an impressive, high-resolution insight into the global climate system, emphasizing both the extreme changes in atmospheric loading over glacial/interglacial time scales and the abrupt nature of millennial scale climate events, with the attendant atmospheric circulation changes that they imply. Despite the large amount of literature on the Chinese loess record, the impression is that the potential of the loess record as a paleoclimate indicator has yet to be fully realized. Much of this relates to the fact that at present the interpretation of the Chinese loess record is constrained, and perhaps misled, by the limited resolution and restricted time cover of current dating techniques. With the advent of more reliable numerical dating techniques, such as the advances that are now taking place in OSL dating, a reliable and appropriate resolution chronology for the loess successions may become more of a reality, providing greater insight into palaeoclimate events.

6. Dust modelling

Understanding the role of dust in the Earth system has prompted intensive development of dust models since the late 1980s. These developments began with modelling 3-D dust transport (Pilinis and Seinfeld, 1987; Westphal et al., 1988). Since then, many regional dust models have been produced and applied to the major wind erosion regions around the world, including Antarctica (Genthon, 1992), the Mediterranean (Nickovic and Dobricic, 1996), the United States (Binkowski and Shankar, 1995), the Saharan desert (Marticorena et al., 1997; Schulz et al., 1998), Australia (Shao and Leslie, 1997; Shao et al., 2007), and Asia (Shao et al., 2003; Uno et al., 2005). There have also been numerous more recent model studies of Saharan dust storms (Pérez et al., 2006; Heinold et al., 2008; Todd, 2008; Menut et al., 2009; Karam et al., 2009; Schepanski et al., 2009; Reinfried et al., 2009; Cavazos et al., 2009; Shao et al., 2010).

With the establishment of the Earth system concept in the 1980s, major climate research centres have developed sophisticated GCMs for climate projections. It became evident that large uncertainties existed in GCM projections partly because of the difficulties in determining the various radiative effects of greenhouse gases and aerosols including dust. Since the 1990s, there has been considerable effort to develop global dust models (Tegen and Fung, 1994, 1995; Zender et al., 2003; Ginoux et al., 2004; Tanaka and Chiba, 2006). Much of our current understanding of global dust cycles and aerosol radiative forcing depends upon these global dust model simulations. Although global dust models are mainly used to simulate time-average dust features, increased model resolution and improved model physics, have enabled their application to simulate individual dust events. Fig. 12 shows a comparison of the MASINGAR (Model for Aerosol Species In the Global Atmosphere, Japan Meteorological Research Institute) simulated atmospheric column dust load for 6 March 2004 and MODIS images. The model simulation has captured the main features of this dust event.

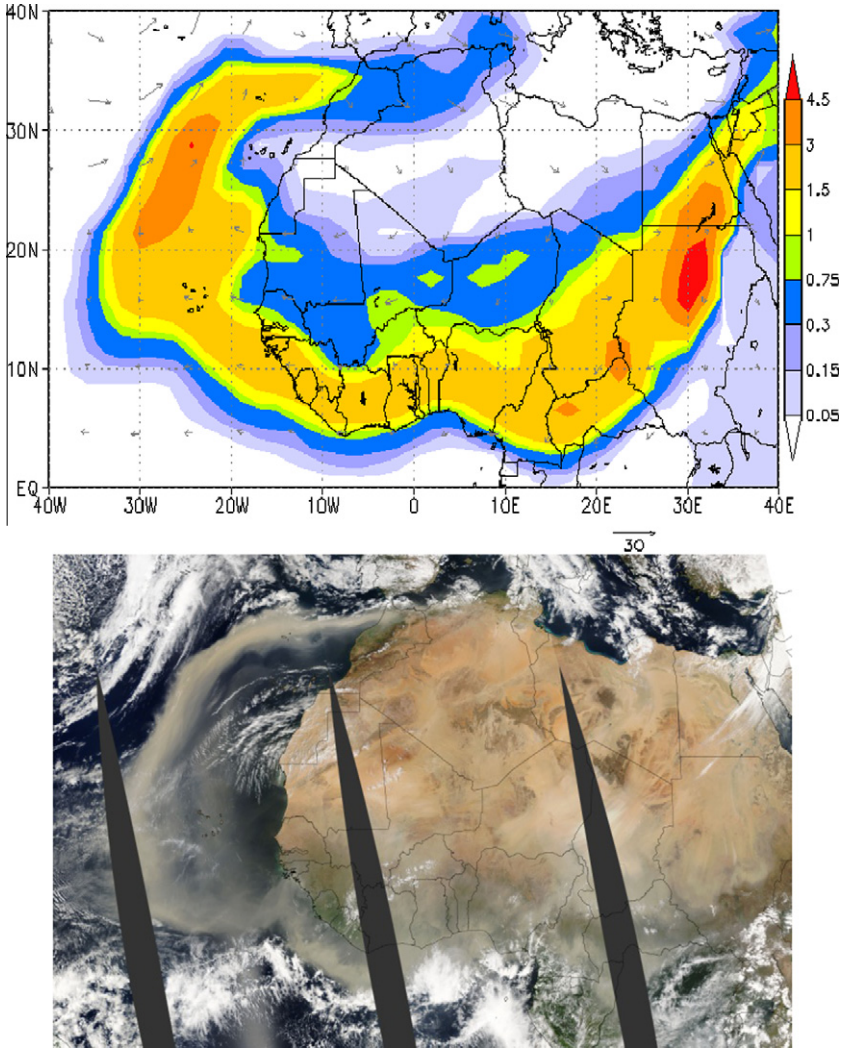

Fig. 12. (a) MASINGAR simulated column dust load in [g m^{-2}] and 700 hPa wind for 12:00UTC 6 March 2004 (Tanaka, 2010 personal communication); (b) Saharan dust storms on 6 March 2004 imaged by MODIS in a series of consecutive overpasses of NASA's Aqua satellite (Image courtesy Jacques Descloitres, MODIS Rapid Response Team, NASA-Goddard Space Flight Center).

The potential of using models to simulate meso-scale dust events has also been tested. Uno et al. (2005) used the RAMS/CFORS model to study the characteristics of dust transport in the Taklimakan with a spatial resolution of 9 km. Their model was able to reproduce the complex flow patterns which produce dust storms in the Tarim Basin, in particular the strong down slope wind from the Tianshan Mountains and the strong easterly flow from the Hexi Corridor. Vogel et al. (2006) also studied the dust transport processes in the Dead Sea area at high spatial resolution (1.58×1.88 km^2).

6.1. Dust emission schemes

Most dust models are integrated systems built on the framework of an atmospheric host model. The latter model includes treatments for atmospheric dynamic and physical processes, such as advection, convection, turbulent diffusion, radiation and clouds, as well as land-, ocean- and ice-surface parameterizations. The dust module of such systems deals with dust emission, transport, deposition and chemistry. For dust modelling, specific parameter data sets are required, which are normally manipulated using a GIS. In general, the dust module starts with solving the dust conservation equation:

$$\frac{\partial c}{\partial t}+\frac{\partial c}{\partial x}+\frac{\partial c}{\partial y}+(w-w_t)\frac{\partial c}{\partial z}=k\nabla^2 c+S_r+S_c \quad (1)$$

where t is time, x and y are horizontal distances and z is height; for different particle size groups, where c is dust concentration, K is particle eddy diffusivity, S_r is wet and dry removal and S_c is dry and moist convection, u, v and w are wind velocity component and w_t is particle terminal velocity. Equation (1) is solved subject to the surface boundary condition

$$\rho(w-w_t)c-\rho k\frac{\partial c}{\partial z}=F_0 \quad (2)$$

where ρ is air density and F_0 is net dust flux at the surface, which is the difference between dust emission and dust deposition.

Dust emission schemes have been proposed, based on micro-physical understanding (Shao et al., 1993; Marticorena and Bergametti, 1995; Alfaro and Gomes, 2001; Shao, 2004). In general, these schemes have produced credible dust emission estimates and are still in use in most regional dust models. The implementation of physics-based dust schemes has encountered considerable difficulties due to the lack of the soil and land-surface parameters. Dust emission is sensitive to several land surface parameters, such as soil moisture and aerodynamic roughness length. The dust emission scheme of Shao (2004) also requires parent soil particle-size

data for the prediction of size-resolved dust fluxes. All these parameters are difficult to obtain with accuracy. There are also concerns about how physics-based dust emission schemes can be scaled up for use in global and regional models. Observations show that for a given wind speed, the rate of dust emission can scatter over orders of magnitude (Shao, 2004). An inter-comparison of dust models shows that the model predictions of dust emission can differ by one order of magnitude (Uno et al., 2006).

Listed in Table 5 are three dust emission schemes. Scheme-I assumes a $F \propto u_*^n$ relationship (with u_* being friction velocity), in which α_g is an empirical coefficient and u_{*_t} is threshold friction velocity. Data shows n falls between 3 and 5, but is often set to 4. The scheme is popular due to its simple formulation, but it is not simple to estimate α_g and there are no guidelines for its specification. The scheme gives an estimate of total dust emission, F, but not particle-size (d_i) resolved dust emission, $F(d_i)$. In practice, F is first computed and then divided into different dust bins provided information is known about the airborne dust particle size distribution $p_{ad}(d)$. Scheme-II assumes that the ratio between dust emission rate and saltation flux, F/Q, is a function of the percentage of clay, η_c. The dimensions of F/Q are [m^{-1}] and a_1, a_2 and a_3 are empirical coefficients. The scheme is not spectral.

In Scheme-III, both saltation bombardment and aggregate disintegration are considered. The scheme is spectral, because $F(d_i, d_s)$, the emission of dust of size d_i generated by the saltation of sand of size d_s, is directly computed. In the scheme, c_y is a coefficient, γ is a weighting function, σ_p is the ratio between free and aggregated dust and σ_m is the bombardment efficiency. The scheme reflects the fact that dust emission is proportional to saltation mass transport, but the proportionality depends on soil texture and binding characteristics. Scheme-III is more complex than the other schemes, but is still very simple. The soil and land-surface data required by the scheme are not yet widely available. In particular there is a need for parent soil particle size distribution. Fig. 13 shows a comparison of Scheme-III simulated dust flux with JADE (Japan-Australia Dust Experiment) in 2006.

6.2. Dust deposition schemes

Dust deposition is even more problematic in terms of monitoring and modelling than dust emission, because:

- there are few networks for dust deposition measurements;
- few measurements have been made in or near dust source regions;
- dry and wet deposition measurement techniques are poorly developed;
- dry deposition mechanisms are not well understood;
- wet deposition involves complex below-cloud scavenging and in-cloud micro-physics; and
- parameter databases required for dust deposition estimates have large uncertainties.

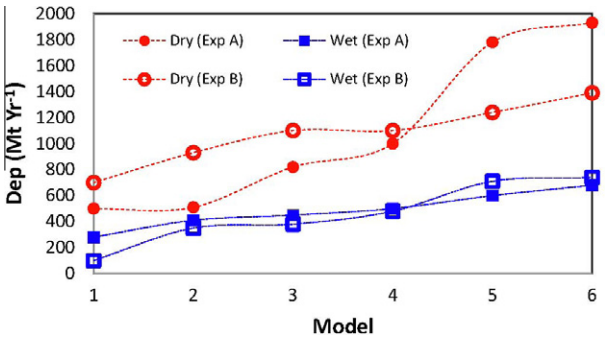

Fig. 14. Inter-comparison of dry and wet depositions for mineral dust as simulated by different global dust models. In Exp-A simulations were done without pre-specifications. In Exp-B simulations were forced with identical dust emission, size distribution and injection height (data from Textor et al., 2006, 2007).

Textor et al. (2006, 2007) analysed global aerosol simulations using diagnostic atmospheric input parameters. Experiments were performed for dust model comparison. In Exp-A, all models worked with no pre-specifications. In Exp-B, dust emission strength, size distribution and dust injection height were specified. Six models were selected for comparison. Fig. 14 shows the model difference in dry and wet deposition. The maximum difference between the models in dry deposition was a factor of 3.7 in Exp-A and 1.9 in Exp-B. For wet deposition, the situation is reversed: the maximum difference was 2.4 in Exp-A, but 6.8 in Exp-B. The results of Textor et al. (2006, 2007) as well as Uno et al. (2006) show that dust models are presently not sufficiently constrained and the uncertainties in dust deposition parameterizations are particularly large.

In dust models, dry deposition dust flux, F_d, is commonly expressed as

$$F_d = -\rho w_d c(z) \tag{3}$$

where $c(z)$ is dust concentration at reference level z and w_d is the dry-deposition velocity which depends on height, surface characteristics, flow properties and particle size. In the atmospheric boundary layer, the mechanisms for vertical dust flux vary with height. In the bulk of this layer, gravitational settling and turbulent diffusion dominate, while in the laminar layer immediately above the surface, gravitational settling and molecular diffusion dominate. The two-layer model of Slinn (1982) is still widely used in dust models. For a smooth surface, the Slinn model leads to:

$$w_d = w_t + \frac{w_{dt} w_{dm}}{w_t + w_{dm} + w_{dt}} \tag{4}$$

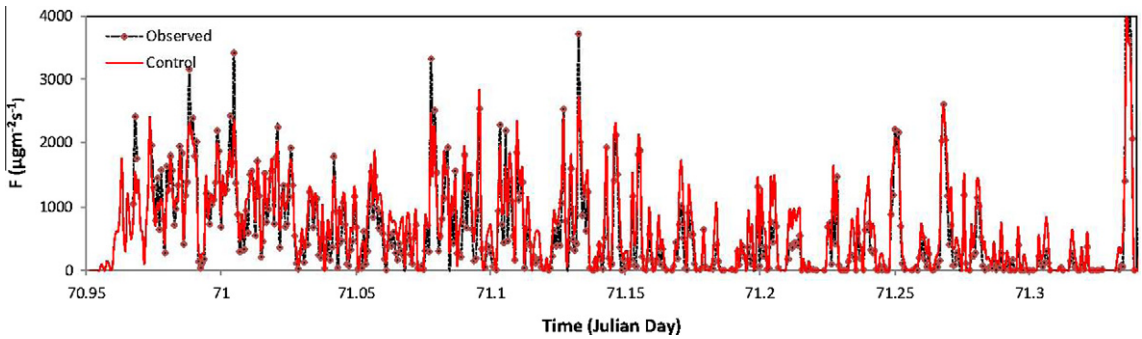

Fig. 13. Time series of Scheme-III simulated and observed dust emission rate on 12 March 2006 at an Australian farm site.

which states that w_d is composed of a gravitational settling velocity w_t and a modification related to the dry-deposition velocity due to turbulence w_{dt} and that due to molecular diffusion w_{dm}. The two-layer approach leaves the possibility open for deriving a model for w_{dm} on the basis of the microscopic physics.

Dry deposition on vegetation involves the transfer of dust by turbulence from air above the canopy to air within the canopy and then by molecular diffusion to vegetation elements. Deposition to the canopy can also be described using the two layer model, but w_{dm} now requires modification. Three mechanisms are commonly considered to control the transfer of dust from canopy air to element surfaces, including molecular diffusion, interception and impaction. Interception occurs due to particle trapping by the fine hairs on vegetation elements or forces arising from static electricity. Impaction occurs because some particles moving in the canopy flow may have a sufficiently large velocity for them to penetrate the laminar flow and impact directly on the surface. These mechanisms can be represented by conductance acting in parallel, so that

$$W_{dm} = w_{dmb} + w_{dmi} + w_{dmm} \tag{5}$$

where w_{dmb}, w_{dmi} and w_{dmm} are the deposition velocities associated with molecular diffusion, interception and impaction. The determination of these velocity components involves complex considerations of boundary layer fluid dynamics (Slinn, 1982). Feng (2008) proposed a similar scheme with more explicit descriptions of the dry-deposition velocity, but there has been no conceptual progress since Slinn (1982).

The dry deposition scheme of Slinn (1982), and the various modifications have been compared with observations collected over different surface types. The essential dependence of w_d on particle size is well captured by the Slinn model, i.e., w_d first decreases and then increases with particle size. The minimum of w_d occurs between 0.1 and 1 μm, although it also depends on flow characteristics. However, comparisons also revealed that the discrepancy between the model and data, and the scatter among the data, could be at least an order of magnitude. Thus, it is extremely difficult to accurately compute the rate of dry deposition in dust models and the differences in dry deposition rates for different types of surfaces are expected to be quite large.

Wet deposition arises due to in-cloud and below-cloud scavenging. In-cloud scavenging refers to the process in which particles act as CCN. Below-cloud scavenging refers to the process in which particles are collected by raindrops as they precipitate. Below-cloud scavenging is simpler and better studied. Scavenging rate, Λ, is the relative decreasing rate of dust-particle number density, *N*:

$$\wedge = -\frac{1}{N}\frac{dN}{dt} = \int_0^\infty (w_R - w_t)\pi(R+r)^2 e_s n_R dR \tag{6}$$

where w_R and w_t are respectively the terminal velocity of raindrops and dust particles of radii R and r, and n_R is the raindrop size distribution function. The particle collection efficiency e_s must be estimated to evaluate Λ. Much effort has been devoted to the details of evaluating this equation. Jung and Shao (2006) compared four such wet deposition schemes.

More often, wet deposition F_w is estimated as:

$$F_w = \rho_w p_{r0} s_0 c_0 \tag{7}$$

In this way, F_w is estimated from precipitation, the scavenging ratio and the airborne dust concentration, all measured at the surface, namely, p_{r0}, s_0 and c_0. Many parameters are contained within s_0, such as particle size, particle shape, the vertical distribution of dust concentration in the atmosphere, the vertical extent of the rain and rain cloud etc. It is therefore difficult to predict its value. The reported s_0 for dust ranges from 100 to 2000 (Uematsu et al., 1985; Duce et al., 1991).

6.3. Data assimilation

Data assimilation techniques combine measurements and model estimates to achieve optimal predictions. These techniques have been successfully applied to atmospheric and oceanic modeling (Kalnay, 2003). Dust concentrations are directly or indirectly observed at surface weather stations (Kurosaki and Mikami, 2005), air-quality monitoring stations, lidar networks (Sugimoto et al., 2003, 2006) and through satellite remote sensing. With increased data availability, there is a marked increase in data-assimilation applications to dust modelling. Yumimoto et al. (2008) used the 4DVAR technique (Chai et al., 2006) to model Asian dust storms, by assimilating the lidar extinction coefficient data into the RAMS/CFORS model for adjoint inversion of dust emission. Ensemble Kalman filters (Sekiyama et al., 2010) are used in conjunction with the MASINGAR model for global dust modeling. The assimilation of the CALIOP/CALIPSO data made possible the modelling of global dust circulation (Fig. 15, Uno et al., 2009).

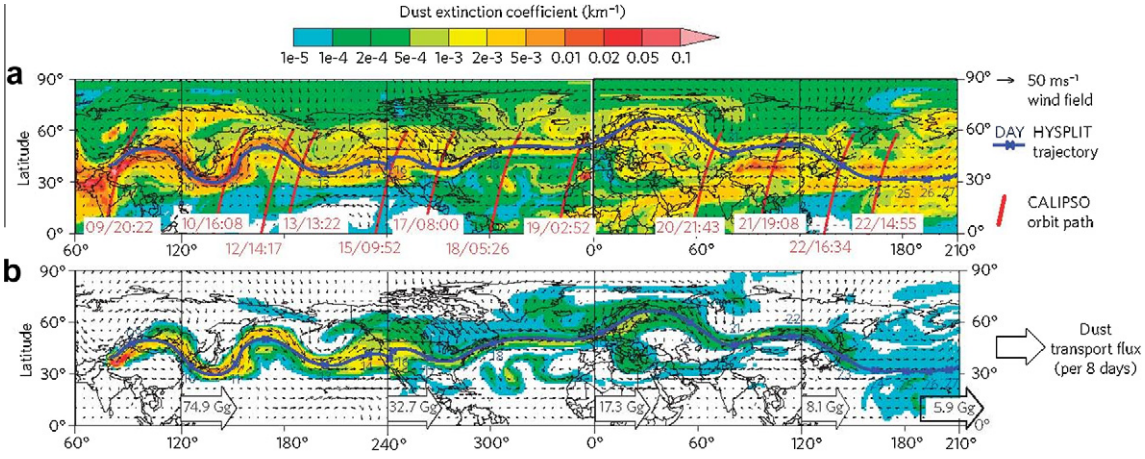

Fig. 15. Distribution of globally transported Asian dust. (a) Dust extinction coefficient (colour) by the model (SPRINTARS) simulation, along with the Lagrangian (HYSPLIT) trajectory (blue solid line). Selected satellite (CALIPSO) orbits (red solid lines) labelled by date (in May 2007)/time. (b) The same as in a, but for the TK1 (Taklamakan dust storm, 8–9 May 2007) simulation. The numbers in the arrows indicate the horizontal dust transport flux crossing each given meridian plane (from Uno et al. 2009).

6.4. Model parameters

A particularly challenging issue in dust modelling is to balance the complexity of dust models, the choice of parameters and the availability of data (Raupach and Lu, 2004). The implementation of physics-based dust emission and deposition schemes has encountered considerable difficulties due to the lack of soil and land-surface parameters. While insufficient work has been done in this area, the recent developments of deriving parameters for dust emission schemes from remote sensing data over extensive areas deserve consideration.

Three categories of parameters can be distinguished based on the different types of dust emission schemes, i.e., parameters which specify (i) soil properties, e.g., soil particle-size distribution and soil-binding strength; (ii) surface aerodynamic roughness properties; (iii) soil thermal and hydraulic properties. These parameters must represent the spatial and temporal variation of the soil surface composition and structure as they control the susceptibility of a soil surface to wind erosion and hence the emission of dust.

Remote sensing of soils has been demonstrated to have considerable potential for the assessment of soil erodibility and soil erosion (Baumgardner et al., 1985; Ben-Dor et al., 1999; Huete and Escadafal, 1991). The main controls on soil surface reflectance variation; organic matter, soil water, mineralogy, particle size and surface roughness are also those that affect the soil surface erodibility by wind. Multi-angular measurements of spectral reflectance provide a useful framework for measuring change at the soil surface) and the surface characteristics can be retrieved using soil bi-directional (spectral) reflectance models and satellite data (Chappell et al., 2006, 2007, 2009).

An important parameter specific to dust emission modelling is the frontal-area index of non-erodible roughness elements. Chappell et al. (2010) proposed to replace this parameter with the proportion of shadow, visible at nadir, integrated for all illumination zenith angles for a particular azimuth angle. The proportion of shadow depends on the geometric anisotropy of the surface roughness in common with the aerodynamic roughness length (z_0). There is a direct relationship between the brightness of the surface roughness of previous studies and their measured z_0 (Fig. 16). There is considerable potential to estimate z_0 frequently over very large areas using SSA of the Earth's surface that is readily measured by medium resolution (200-300m pixels) multi-angle reflectance sensors on airborne and satellite platforms.

7. Dust observation

Global dust activities are traditionally monitored through the network of weather stations distributed around the world. This is a powerful data set, because for some of the dust prone areas, dust weather observations have been continuous for more than 50 years. A dust weather climatology is now well established through the analysis of synoptic dust weather records (McTainsh et al., 2005; Shao and Dong, 2006; Klose et al., 2010; O'Loingsigh et al., 2010). The disadvantage of dust weather data is the relatively sparse distribution of weather stations in key source areas, such as the central Sahara, the Gobi and Taklimakan Deserts and central Australia, plus low and often variable frequencies of observation times.

With the advancement in remote sensing technology and the establishment of air quality monitoring networks, a revolution in dust monitoring has been taking place in recent years. Quantitative and three-dimensional dust observations with high-spatial and temporal resolutions are increasingly made by a combination of data from satellites, lidar networks, deployed radiometers, air samplers and weather stations.

7.1. Remote sensing

Sensors on board satellites detect the radiances of various types from the Earth to allow the monitoring of extensive dust events, the potential to identify dust hot-spots, to derive land-surface parameters required for dust modelling and to derive dust-related entities such as optical thickness, particle size etc. TOMS (1983–2004 except May 1993–Jul 1996) and OMI (2004) have long provided an aerosol index for dust measurement. Recently employed active remote-sensing technology has enhanced the capacity of satellites in dust quantification (Fig. 17). CALIPSO/CALIOP measures aerosol extinction coefficient and SSA to allow for the quantification of aerosol profile with a 30 m vertical resolution and 70 m horizontal resolution.

At the same time, a ground-based global network of about 105 lidars (The Global Atmosphere Watch Aerosol Lidar Observation

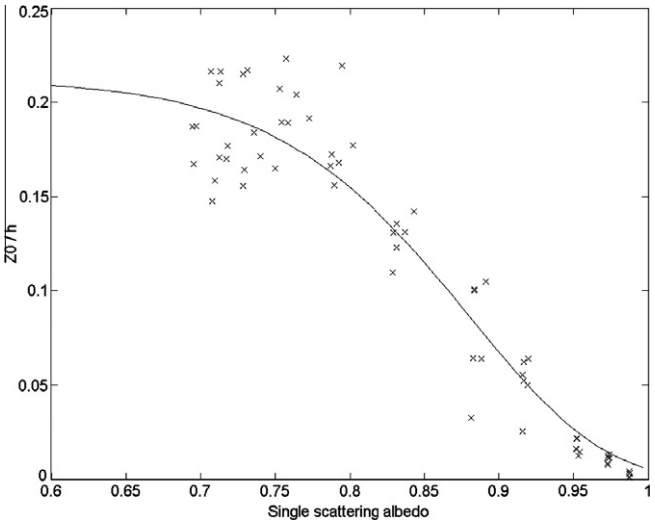

Fig. 16. Model fitted to the single scattering albedo (SSA) of Dong et al. (2002) reconstructed wind tunnel surface roughness and its relationship with the measured aerodynamic roughness length ($z0$) standardized by object height (h).

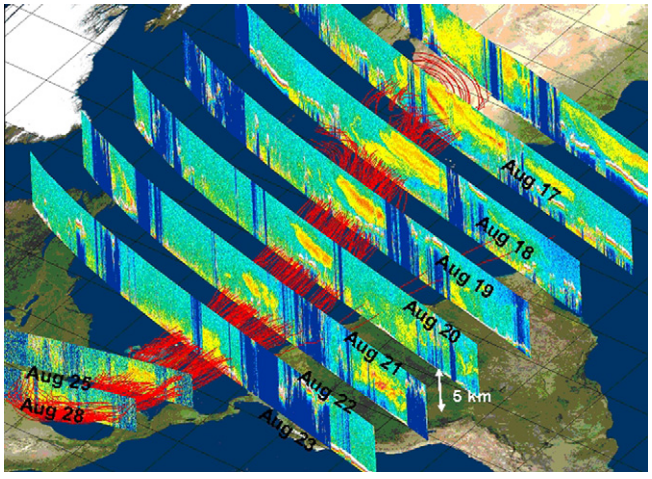

Fig. 17. An example of Calipso's identification of cloud and dust features in August 2007, which allows the determination of their altitude and different particle types. Dust particles originated from the Sahara desert on 17 August were found to drift from Africa to the Gulf of Mexico (from Liu et al. 2008). Red lines represent back trajectories of the dust track. Vertical images are 532 nm attenuated backscatter coefficients measured by CALIOP when passing over the dust track.

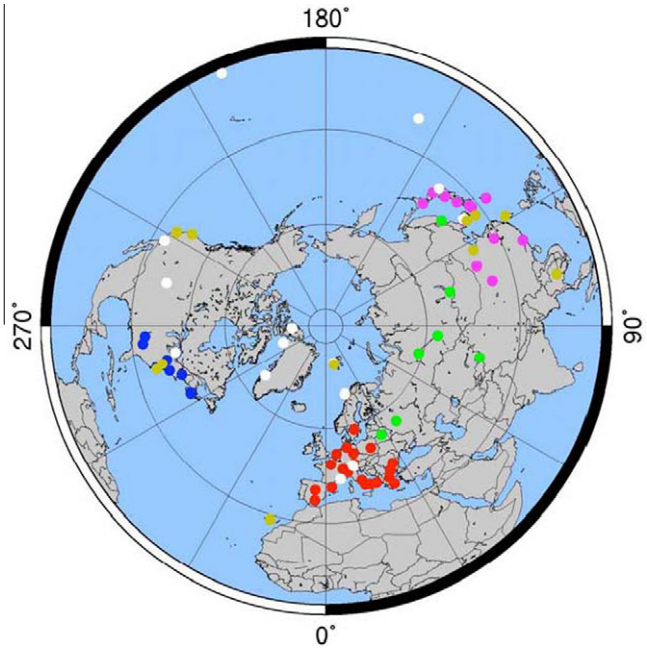

Fig. 18. GALION, a ground-based global network of lidars as available through the cooperation between existing networks (Bösenberg and Hoff, 2008). The different networks are indicated by the dot color: AD-NET (Asian Dust Net) violet, ALINE 8 American Lidar Network) yellow, CISLiNet (CIS Lidar Network) green, EARLINET (European Aerosol Research Lidar Network) red, MPLNET (NASA Micro-Pulse Lidar Network) brown, NDACC (Network for the Detection of Atmospheric Composition Change) white, REALM (Regional East Aerosol Lidar Mesonet) blue.

Network, GALION, Fig. 18) is being established (Bösenberg and Hoff, 2008). GALION builds upon several existing regional lidar networks in Europe, America and Asia. The aerosol properties to be observed through GALION include the identification of aerosol layers and profiles, optical properties, aerosol types as well as microphysical properties. Also AERONET provides globally distributed observations of spectral aerosol optical depths. AERONET has been operating since 1993 and has been carrying out routine measurements at around 150 stations distributed globally. The combination of satellite and ground based networks, such as GALION and AERONET, provides an extremely powerful tool for monitoring the global dust cycle.

7.2. Field measurements

Reliable field data of dust emission and deposition processes for model validation are extremely valuable. Much improved field experiments have been recently carried out to study the physics of wind erosion, in particular size resolved sand fluxes and dust fluxes. For example, Mikami, Ishizuka and Leys organised JADE in Feb–Mar 2006. They measured a wide range of wind-erosion related quantities on an Australian farm, including atmospheric variables (wind, precipitation, etc.), land surface properties (moisture, crustiness etc.), soil particle-size distributions and size-resolved saltation fluxes and dust fluxes. The dataset is the most cohesive and comprehensive field-scale wind-erosion dataset collected so far and provides a solid reference for the validation of size-resolved dust schemes (Ishizuka et al., 2009).

Fig. 19 shows the design and instrumentation of JADE. Saltation flux densities were measured using Saltation Particle Counters (Yamada et al., 2002) of different particle sizes at 0.05, 0.1 and 0.3 m above the ground surface at a sampling rate of 1 Hz. The particle-size range between 38.9 and 654.3 μm was divided into 32 bins with mean diameters of 38.9, 54.1, 69.2 μm, etc. At each

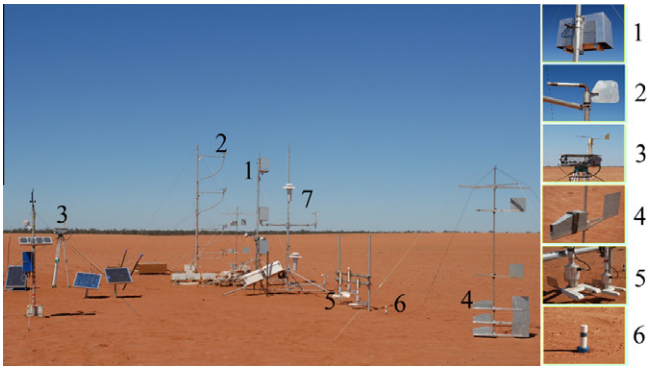

Fig. 19. An example for the set up of a wind-erosion monitoring system in field. Dust concentrations and sizedistributions are measured using Optical Particle Counters (1, OPC at 1, 2 and 3.5 m); TSP concentrations are measured using high-volume air samplers (2, TSP at 1, 2, 3.5 and 5 m) and PM10 concentrations are measured using a Dust Track (3, at 2m); Saltation flux is measured using an array of Fryrear sand traps (4, at 0.1, 0.2, 0.5, 1 and 2 m), Sand Particle Counters (5, SPC at 0.05, 0.1 and 0.3m) and a Sensit (6, at 0.1 m). It also consists of a micro-meteorological station for recording wind profiles and other meteorological data (7, AWS). (Experiment set up by M Mikami, J F Leys and M Ishizuka).

measurement height, q (saltation flux density, $ML^{-2}T^{-1}$) was obtained as the sum of q_i (saltation flux density of size bin (i) for the 32 size bins. Optical Particle Counters (OPC) were used to measure dust concentration of the following 8 size groups: 0.3–0.6, 0.6–0.9, 0.9–1.4, 1.4–2.0, 2.0–3.5, 3.5–5.9, 5.9–8.4 and >8.4 μm at heights 1, 2 and 3.5 m. From the dust profile measurements, dust fluxes of these size groups could be derived. Such data sets are extremely valuable for the verification of wind-erosion and dust-emission models.

8. Concluding remarks

Despite the remarkable progress made in dust research over the past three decades or so, many challenges remain. There is only scope in this review for us to focus on the main issues.

8.1. Quantification of dust cycle

The dust cycle is poorly quantified when compared with other Earth cycles. Recent model estimates of global dust emission (and hence dust deposition) are converging to 2000 Mt yr^{-1}, but this convergence does not necessarily represent greater accuracy. There are no data at the global scale for direct validation of modelled dust emission, deposition and particle size. The only data available are dust concentration estimates retrieved from satellite data and air quality monitoring stations and these are rarely rigorously correlated. Currently there is no global dust model with the capacity to predict dust particles-size distributions. Furthermore, as the studies of Uno et al. (2006) and Textor et al. (2006, 2007) demonstrate, the uncertainties in dust models remain potentially large and unquantified.

Dust emission schemes used in dust models are those developed in the 1990s. The nature of the schemes is deterministic while dust emission is affected by a wide range of factors which should be considered as stochastic. Progress on dust emission parameterization in more recent years has been slow. New developments in theory and experiments are needed to better understand and describe the stochastic nature of dust emission. Dust deposition schemes are even more problematic. There has been no significant conceptual progress since the 1980s and the disagreement between predicted and wind-tunnel observed dry deposition velocity between schemes is easily one order of magnitude. Large uncertainties exist in the treatments of both

aerodynamic transfer of dust particles through the atmospheric surface layer and the surface collection efficiency.

An urgent issue is to establish benchmark data sets for validation of dust emission and deposition schemes. Despite the recent improvements in the strategies and techniques for dust observations in field and wind-tunnel experiments, the research community does not yet have a benchmark test dataset necessary for the development of dust parameterization schemes.

Dust emission and deposition schemes are based on point-scale micro physics, while regional and global dust models require their implementation at scales of 10s to 100s of kilometers. The upscaling of point-scale micro physics to regional scale dust flux estimates poses a major challenge in the quantification of the dust cycle. The problem of upscaling is not unique to dust modeling, but common to many areas in Earth system studies and much can be learned from related study areas, such as the upscaling techniques used in land-surface parameterization. The upscaling procedure requires well established parameter databases for the entire globe. The databases for global land surface modeling are well established and continuously improved, in contrast to dust modeling, where a common set of parameters is yet to be agreed upon and a process of compiling dust-dedicated databases yet to be initiated.

The accurate simulation of meteorological conditions remains a critical issue for the quantification of the dust cycle. Timmreck and Schulz (2004) and Menut (2008) showed that dust emission is sensitive to the way winds are represented in dust models. In particular, meso-scale atmospheric systems which are mostly unresolved in global and regional dust models are often responsible for intense dust emissions, such as haboobs (Knippertz et al., 2007), gusty winds (Engelstaedter and Washington, 2007), low-level jets (Schepanski et al., 2009), dust devils and convective turbulence (Klose et al., 2010). The downscaling of global and regional flow patterns to meso-scale and micro-scale dust flux estimates deserves particular attention.

Attention also needs to be paid to the nature and rate of weathering processes and their role in dust supply. Dust emission is generally supply-limited, and the quantity and rate of dust supply to aeolian processes depends on the nature and rate of weathering. For example, a cold winter over the Gobi and adjacent steppe lands can dramatically increase dust supply to Asian dust storms in the following spring, yet there is little detailed information available on these processes.

The stratigraphic record has much to offer in better understanding and quatifying the global dust cycle, but this can only be achieved if its interpretation is placed within the context of contemporary process and modelling work. While such issues of secure age-control remain, it has become possible to move on from traditional descriptive interpretations and place questions into a more quantitative and process-based context. A number of modelling studies have already demonstrated the advantages of such an approach, but much more can be achieved, especially through the perspective offered by regional models.

8.2. Dust feedbacks

There is considerable uncertainty in the estimates of dust radiative forcing, largely due to a shortage of data on dust particle-size distributions, particle shape, elemental composition and in particular mineralogy; all of which affect dust optical properties. Existing dust models do not have sufficient skill in predicting, for example, the size distribution and mineralogical composition of dust during emission and the subsequent mixing and chemical reaction with anthropogenic and biogenic pollutants as well as salt. Transformations in physical, chemical and optical properties of dust particles can be quite large, but there is so far a critical lack of observational data for studying these during dust transportation.

Dust appears to generate feedbacks in the Earth system on various scales e.g. the dust-CO_2 feedback (iron hypothesis) on geological time scales and the dust-ABLS (atmospheric boundary layer stability) feedback on diurnal time scales. Both are negative feedbacks. There are other feedbacks on synoptic to annual time scales, which are of particular interest to the climate modelling community. It is challenging to quantify the strength and to demonstrate the mechanisms of dust related feedbacks. Feedbacks reported in the existing literature need to be substantiated.

8.3. Dust iron

The "iron-hypothesis" has attracted much attention. However, the limiting effect of iron to ocean phytoplankton activity is conditioned, depending on whether ocean waters are LNLC or HNLC. While the iron hypothesis appears to be strongly supported at geological time scales there are many gaps in our process knowledge of the inter-relationships between the dust cycle and the iron cycle. For example, while it is common knowledge that the iron required for phytoplankton growth must be Fe^{2+}, there are few measurements that show how Fe^{3+} in dust may be reduced to Fe^{2+} as dust propagates through clouds or anthropogenically polluted air masses.

8.4. Wind and water erosion

The connection between aeolian and fluvial processes has been discussed on several occasions in this paper. It should be re-emphasised that the emission and transport processes of mineral sediments, chemical species and organic matter in the Earth system are carried out jointly by air and water. The transport of carbon by wind and water in the Earth system provides a typical example. Soil is the largest terrestrial reservoir of mobile carbon; with three times the quantity of atmospheric carbon and five times that of continental biosphere carbon. Soil organic carbon (SOC) is concentrated in topsoils and the transport of SOC by wind and water directly affects the global carbon budget. Because the preservation of SOC is important to land use sustainability, there have been numerous tillage-scale monitoring and modelling studies on the redistribution of carbon by water, but the role of wind erosion in redistributing carbon rich fine material has not been thoroughly investigated. Given the organic matter winnowing potential of aeolian entrainment, filling this knowledge gap may make a significant contribution to our understanding of how the dust cycle and carbon cycle interact and affect climate.

Two overaching themes have been identified from our review: (i) the strengthening of the global dust perpective, best accommodated in the concept of the dust cycle; and (ii) the importance of predictive models at a range of spatial and temporal scales. Both themes bring as a goal the integration of dust research with the development of Earth system models and the emergence of the global dust cycle as a core subject in Earth system sciences. The central issue which now prompt us is to give focus to the development of a new generation of dust models based on the global dust cycle concept, supported by the new observationa, new observational techniques and computational methods. This approach will provide us with a powerful tool to better understand and to quantify the role of dust in the Earth system and the interactions between the dust, carbon and energy cycles, both in the past, at the preent and in future.

References

Alfaro, S.C., Gomes, L., 2001. Modelling mineral aerosol production by wind erosion: Emission intensities and aerosol size distributions in source areas. J. Geophys. Res. 106, 18075–18084.

Alley, R.B., Meese, D.A., Shuman, C.A., Gow, A.J., Taylor, K.C., Gootes, P.M., White, J.M.C., Ram, M., Waddington, E.D., Mayewski, P.A., Zielinski, G.A., 1993. An abrupt increase in Greenland snow accumulation at the end of the Younger Dryas event. Nature 362, 527–529.
An, Z., 2000. The history and variability of the East Asian paleomonsoon climate. Quat. Sci. Rev. 19, 171–187.
Andreae, M.O., Rosenfeld, D., 2008. Aerosol–cloud–precipitation interactions. Part 1 the nature and sources of cloud-active aerosols. Earth-Sci. Rev. 89, 13–41.
Aoki, T., Tanaka, T.Y., Uchiyama, A., Chiba, M., Mikami, M., Yabuki, S., Key, J.R., 2005. Sensitivity experiments of direct radiative forcing caused by mineral dust simulated with a chemical transport model. J. Meteorol. Soc. Japan 83A, 315–331.
Aoki, T., Motoyoshi, H., Kodama, Y., Yasunari, T.J., Sugiura, K., Kobayashi, H., 2006. Atmospheric aerosol deposition on snow surfaces and its effect on albedo. SOLA 2, 13–16. doi:10.2151/sola.2006-3004.
Arimoto, R., Kim, Y.J., Kim, Y.P., Quinn, P.K., Bates, T.S., Anderson, T.L., Gong, S., Uno, I., Chin, M., Huebert, B.J., Clarke, A.D., Shinozuka, Y., Weber, R.J., Anderson, J.R., Guazzotti, S.A., Sullivan, R.C., Sodeman, D.A., Prather, K.A., Sokolik, I., 2006. Characterization of Asian dust during ACE-Asia. Global Planet. Changes 52, 23–56.
Barker, S., Knorr, G., 2007. Antarctic climate signature in the Greenland ice core record. Proc. Natl. Acad. Sci. USA 104 (44), 17178–17282.
Baumgardner, M.F., Silva, L.F., Biehl, L.L., Stoner, E.R., 1985. Reflectance properties of soils. Adv. Agronomy 38, 1–44.
Ben-Dor, E., Irons, J.R., Epema, G., 1999. Soil reflectance. In: Renzc, A.N. (Ed.), Remote Sensing for the Earth Sciences, vol. 3. New York, Wiley, pp. 111–188.
Binkowski, F.S., Shankar, U., 1995. The regional particulate matter model 1. Model description and preliminary results. J. Geophys. Res. 100, 26191–26209.
Biscaye, P.E., Grousset, F.E., Revel, M., Van der Gaast, S., Zielinski, G.A., Vaars, A., Kukla, G., 1997. Asian provenance of glacial dust (stage 2) in the Greenland Ice Sheet Project 2 Ice Core, Summit. Greenland J. Geophys. Res. 102, 26765–26781.
Bösenberg, J., Hoff, R.M., 2008. GALION, The GAW Atmospheric Lidar Observation Network. WMO GAW Report. World Meterological Organization/Global Atmosphere Watch, Geneva, Switzerland.
Bou Karam, D., Flamant, C., Knippertz, P., Reitebuch, O., Pelon, J., Chong, M., Dabas, A., 2008. Dust emission over the Sahel associated with the West African monsoon intertropial discontinuity region: a representative case-study. Q. J. R. Meteorol. Soc. 134, 621–634.
Bradley, R.S., 1999. Paleoclimatology: Reconstructing Climates of the Quaternary. Harcourt-Academic Press, 613pp.
Budyko, M., 1969. The effect of solar radiation variations on the climate of the Earth. Tellus 21, 611–619.
Bullard, J.E., McTainsh, G.H., 2003. Aeolian–fluvial interactions in dryland environments: examples, concepts and Australia case study. Prog. Phys. Geogr. 27, 359–389.
Bullard, J.E., McTainsh, G.H., Pudmenzky, C., 2007. Factors affecting the nature and rate of dust production from natural dune sands. Sedimentology 54, 169–182.
Bush, B.C., Valero, F.P.J., 2003. Surface aerosol radiative forcing at Gosan during the ACE-Asia campaign. J. Geophys. Res. 108, 8660. 10.1029/2002JD003233.
Cavazos, C., Todd, M.C., Schepanski, K., 2009. Numerical model simulation of the Saharan dust event of 6-11 March 2006 using the Regional Climate Model version 3 (RegCM3). J. Geophys. Res. 114, D12109. 10.1029/2008JD011078.
Chai, T.F., Carmichael, G.R., Sandu, A. et al., 2006. Chemical data assimilation of Transport and Chemical Evolution over the Pacific (TRACE-P) aircraft measurements. J. Geophys. Res. 111 (D2): Art. No. D02301.
Chapin III, F.S., Sturm, M., Serreze, M.C., McFadden, J.P., Key, J.R., Lloyd, A.H., McGuire, A.D., Rupp, T.S., Lynch, A.H., Schimel, J.P., Beringer, J., Chapman, W.L., Epstein, H.E., Euskirchen, E.S., Hinzman, L.D., Jia, G., Ping, C.L., Tape, K.D., Thompson, C.D.C., Walker, D.A., Welker, J.M., 2005. Role of land surface changes in Arctic summer warming. Science 310, 657–660.
Chappell, A., Zobeck, T., Brunner, G., 2006. Using bi-directional soil spectral reflectance to model soil surface changes induced by rainfall and wind-tunnel abrasion. Remote Sens. Environ. 102 (3–4), pp. 328–343. Avialable from: http://dx.doi.org/10.1016/j.rse.2006.02.020.
Chappell, A., Strong, C., McTainsh, G.H., Leys, J.F., 2007. Detecting induced in situ erodibility of a dust-producing playa in Australia using a bi-directional soil spectral reflectance model. Rem. Sens. Environ. 106, pp. 508–524. Available from: http://dx.doi.org/10.1016/j.rse.2006.09.009.
Chappell, A., Leys, J.F., McTainsh, G.H., Strong, C., Zobeck, T., 2009. Simulating Multi-angle Imaging Spectro-Radiometer (MISR) sampling and retrieval of soil surface roughness and composition changes using a bi-directional soil spectral reflectance model. In: Hill, J., Röder, A. (Eds.), Advances in Remote Sensing and Geoinformation Processing for Land Degradation Assessment. Taylor and Francis.
Chappell, A., Van Pelt, S., Zobeck, T., Dong, Z., 2010. Estimating aerodynamic resistance of rough surfaces using angular reflectance. Rem. Sens. Environ. 114, pp. 1462–1470. Available from: http://dx.doi.org/10.1016/j.rse.2010.01.025.
Chen, L., Yin, Y., Yang, J., Niu, S., 2007. Effects of sand dust particles on cloud and precipitation: a numerical study. J. Nanjing Inst. Met. 30, 590–600.
Chin, M., Ginoux, P., Kinne, S., Torres, O., Holben, B.N., Duncan, B.N., Martin, R.V., Logan, J.A., Higurashi, A., Nakajima, T., 2002. Tropospheric aerosol optical thickness from the GOCART model and comparisons with satellite and sun photometer measurements. J. Atmos. Sci. 59, 461–483.
Clarke, A.D., Noone, K.J., 2007. Soot in the arctic snowpack: a cause for perturbations in radiative transfer. Atmos. Environ. 41, 64–72. doi:10.1016/j.atmosenv.2007.10.059.
Collins, W.D., Conant, W.C., Ramanathan, V., 1994. Earth radiation budget, clouds and climate sensitivity. In: Calvert, J.G. (Ed.), The Chemistry of the Atmosphere: Its Impact on Global Change. Blackwell Scientific Publishers, Oxford, pp. 207–215.
Cronin, T.M., 2009. Paleoclimates: Understanding Climate Change Past and Present. Columbia University Press, New York. 441pp.
Crutzen, P.J., Stormer, E.F., 2000. The "Anthropocene". IGBP Newsletter 41, 12–14.
D'Almeida, G.A., 1986. A model for Saharan dust transport. J. Climate Appl. Met. 25, 903–916.
D'Almeida, G.A., 1987. Desert aerosol characteristics and effects on climate. In: Leinen, M., Sarnthein, M. (Eds.), Palaeoclimatology and Palaeometeorology: Modern and Past Patterns of Global Atmospheric Transport. NATO ASI Series C. Springer Verlag, Berlin, pp. 311–338.
Dansgaard, W., Johnsen, J., Moller, I., Langway, C.C., 1969. One thousand centuries of climate record from Camp Century on the Greenland Ice Sheet. Science 166, 377–381.
Dansgaard, W., Clausen, H.B., Gundestrup, N., Hammer, C.U., Johnson, S.F., Kristinsdottir, P.M., Reeh, N., 1982. A new Greenland deep ice core. Science 218, 1273–1278.
Delmonte, B., Basile-Doelsch, I., Petit, J.R., Maggi, V., Revel-Rolland, M., Michard, A., Jagoutz, E., Grousset, F., 2005. Comparing the Epica and Vostok dust records during the last 220,000 years: stratigraphical correlation and provenance in glacial periods. Earth-Sci. Rev. 66, 63–87.
Delmonte, B., Andersson, P.S., Schönberg, H., Hansson, M., Petit, J.R., Delmas, R., Gaiero, D.M., Maggi, V., Frezzotti, M., 2010. Geographic provenance of aeolian dust in East Antarctica during Pleistocene glaciations: preliminary results from Talos Dome and comparison with East Antarctic and new Andean ice core data. Quaternary Sci. Rev. 29, 256–264.
Derbyshire, E., 2003. Loess and the dust indicators and records of terrestrial and marine palaeoenvironments (DIRTMAP) database. Quaternary Sci. Rev. 22, 18–19.
Ding, Z.L., Yu, Z.W., Rutter, N.W., Liu, T.S., 1994. Towards an orbital time scale for Chinese loess. Quaternary Sci. Rev. 13, 39–70.
Ding, Z.L., Yu, Z.W., Yang, S.L., Sun, J.M., Xiong, S.F., Liu, T.S., 2001. Coeval changes in grain size and sedimentation rate of eolian loess, the Chinese Loess Plateau. Geophys. Res. Lett. 28 (10), 2097–2100.
Dong, Z., Liu, X., Wang, X., 2002. Aerodynamic roughness of gravel surfaces. Geomorphology 43(1–2), 532 17–31.
Dubovik, O., Holben, B.N., Eck, T.F., Smirnov, A., Kaufman, Y.J., King, M.D., Tanré, D., Slutsker, I., 2002. Variability of absorption and optical properties of key aerosol types observed in worldwide locations. J. Atmos. Sci. 59, 590–608.
Duce, R.A., Liss, P.S., Merrill, J.T., et al., 1991. The atmospheric input of trace species to the world ocean. Global Biogeochem. Cycles 5, 193–259.
Engelstaedter, S., Washington, R., 2007. Atmospheric controls on the annual cycle of North African dust. J. Geophys. Res. 112, D03103. doi:10.1029/2006JD007195.
Feng, J., 2008. A size-resolved model and a four-mode parameterization of dry deposition of atmospheric aerosols. J. Geophys. Res. 113, D12201. doi:10.1029/2007JD009004.
Fischer, H., Siggard-Andersen, R.U., Röthlisberger, R., Wolff, E., 2007. Glacial/interglacial changes in mineral dust and sea-salt records in polar ice cores: sources, transport and deposition. Rev. Geophys. 45, RG1002. doi:10.1029/2005RG000192.
Fuhrer, K., Wolff, E.W., Johnsen, S.J., 1999. Timescales for dust variability in the Greenland Ice Core Project (GRIP) ice core in the last 100,000 years. J. Geophys. Res. 104 (D24), 31043–31052.
Gabrielli, P., Wegner, A., Petit, J.R., Delmonte, B., De Deckker, P., Gaspari, V., Fischer, H., Ruth, U., Kriews, M., Boutron, C., Cescon, P., Barbante, C., 2010. A major glacial-interglacial change in aeolian dust composition inferred from Rare Earth Elements in Antarctic ice. Quat. Sci. Rev. 29, 265–273.
Gangoiti, G., Alonso, L., Navazo, M., García, J.A., Millán, M., 2006. North African soil dust and European pollution transport to America during the warn season: hidden links shown by a passive tracer simulation. J. Geophys. Res. 111, D10109. doi:10.1029/2005JD00594.
Gao, Y., Arimoto, R., Duce, R.A., Zhang, X.Y., Zhang, G.Y., An, Z.S., Chen, L.Q., Zhou, M.Y., Gu, D.Y., 1997. Temporal and spatial distributions of dust and its deposition to the China Sea. Tellus 49B, 172–189.
Genthon, C., 1992. Simulations of desert dust and sea salt aerosols in Antarctic with a general circulation model of the atmosphere. Tellus 44, 371–389.
Ginoux, P., Chin, M., Tegen, I., Prospero, J., Holben, B., Dubovik, O., Lin, S.J., 2001. Sources and distribution of dust aerosols simulated with the gocart model. J. Geophys. Res. 106, 20255–20273.
Ginoux, P., Prospero, J.M., Torres, O., Chin, M., 2004. Long-term simulation of dust distribution with the GOCART model: Correlation with the North Atlantic Oscillation. Environ. Mod. Software 19, 113–128.
Grini, A. et al., 2005. Model simulations of dust sources and transport in the global atmosphere: Effects of soil erodibility and wind speed variability. J. Geophys. Res. 110, D02205.
Guo, Z.T., Ruddiman, W.F., Hao, Q.Z., Wu, H.B., Qiao, Y.S., Zhu, R.X., Peng, S.Z., Wei, J.J., Yuan, B.Y., Liu, T.S., 2002. Onset of Asian desertification by 22 Myr ago inferred from loess in China. Nature 416, 159–163.
Haberlah, D., Williams, M.A.J., Halverson, G., Hill, S.M., Hrstka, T., Butcher, A.R., McTainsh, G.H., Glasby, P., 2010. Loess and floods: high resolution multi-proxy data of Last Glacial Maximum (LGM) slackwater deposition in the Flinders Ranges, semi-arid South Australia. Quaternary Sci. Rev. 29, 2673–2693. doi:10.1016/j.quascirev.2010.04.014.

Han, Y.X., Chen, Y., Fang, X., Zhao, T., 2008. The possible effect of aerosol on precipitation in Trim basin. China Environ. Sci. 28, 102–106.
Hand, J.L., Mahowald, N.M., Chen, Y., Siefert, R.L., Luo, C., Subramaniam, A., Fung, I., 2004. Estimates of atmospheric-processed soluble iron from observations and a global mineral aerosol model: Biogeochemical implications. J. Geophys. Res. 109, D17205, doi:10.1029/2004JD004574.
Hao, Q., Guo, Z., 2007. Magnetostratigraphy of an early-middle Miocene loess-soil sequence in the western Loess Plateau of China. Geophys. Res. Lett. 34, L18305. doi:10.1029/2007GL031162.
Haywood, J.M., Allan, R., Culverwell, I., Slingo, T., Milton, S., Edwards, J., Clerbaux, N., 2005. Can desert dust explain the outgoing longwave radiation anomaly over the Sahara during July 2003? J. Geophys. Res. 110, D05105. doi:10.1029/2004JD005232.
Heinold, B., Tegen, I., Schepanski, K., Hellmuth, O., 2008. Dust radiative feedback on Saharan boundary layer dynamics and dust mobilization. Geophys. Res. Lett. 35, L20817. doi:10.1029/2008GL035319.
Heller, F., Liu, T.S., 1982. Magnetostratigraphical dating of loess deposits in China. Nature 300, 431–433.
Hesse, P., 1994. The record of continental dust from Australia in Tasman Sea sediments. Quaternary Sci. Rev. 13, 257–272.
Hesse, P., McTainsh, G.H., 1999. Last glacial maximum to early Holocene wind strength in the mid-latitudes of the Southern Hemisphere from aeolian dust in the Tasman Sea. Quaternary Res. 52, 343–349.
Holben, B.N., Tanre, D., Smirnov, A., Eck, T.F., Slutsker, I., Abuhassa, N., Newcomb, W.W., Schafer, J.S., Chatenet, B., Lavernu, F., Kaufman, Y.J., Vande Castle, J., Setzer, A., Markham, B., Clark, D., Rouin, R., Halthore, R., Karneli, A., O'Neil, N.T., Piertras, C., Pinker, R.T., Voss, K., Zibordi, G., 2001. An emerging ground-based aerosol climatology: aerosol optical depth from AERONET. J. Geophys. Res. 106, 12067–12097.
Hovan, S.A., Rea, D.K., Pisias, N.G., Shackleton, N.J., 1989. A direct link between the China loess and marine $\delta^{18}O$ records: aeolian flux to the north Pacific. Nature 340, 296–298.
Huang, J., Wang, Y., Wang, T., Yi, Y., 2006a. Dusty cloud radiative forcing derived from satellite data for middle latitude region of East Asia. Prog. Natural Sci. 10, 1084–1089.
Huang, J., Lin, B., Minnis, P., Wang, T., Wang, X., Hu, Y., 2006c. Yi. Y, Ayers, J.R..
Huang, J., Minnis, P., Lin, B., Wang, T., Yi, Y., Hu, Y., Sun-Mack, S., Ayers, K., 2006b. Possible influences of Asian dust aerosols on cloud properties and radiative forcing observed from MODIS and CERES. Geophys. Res. Lett. 33, L06824. doi:10.1029/2005GL024724.
Huang, J., Fu, Q., Su, J., Tang, Q., Minnis, P., Hu, Y., Yi, Y., Zhao, Q., 2009. Taklimakan dust aerosol radiative heating derived from CALIPSO observations using the Fu-Liou radiation model with CERES constraints. Atmos. Chem. Phys. 9, 4011–4021.
Huebert, B.J., Bates, T., Russell, P.B., Shi, G., Kim, Y.J., Kawamura, K., Carmichael, G., Nakajima, T., 2003. An overview of ACE-Asia:Strategies for quantifying the relationships between Asian aerosols and their climatic impacts. J. Geophys. Res., 108. doi:10.1029/ 2003JD003550.
Huete, A.R., Escadafal, R., 1991. Assessment of biophysical soil properties through spectral decomposition techniques. Rem. Sens. Environ. 35, 149–159.
Hyeong, K., Park, S.H., Yoo, C.M., Kim, K.H., 2005. Mineralogical and geochemical composition of the eolian dust from the northeast equatorial Pacific and their implications on paleolocation of the Intertropical Convergence Zone. Paleoceanography 20, PA1010, doi:1029/2004PA001053.
IPCC, 2007. Climate Change 2007: The Physical Basis. In: Solomon, S., Qin, D., Manning, M., Chen, Z., Marquis, M., Averyt, K.B., Tignor, M., Miller, H.L. (Eds.), Contribution of the Working Group I to the Fourth Assessment Report of the Intergovernmental Panel on Climate Change. Cambridge University Press, Cambridge, United Kingdom.
Ishizuka, M., Mikami, M., Leys, J.F., Yamada, Y., Heidenreich, S., Shao, Y., McTainsh, G.H., 2008. Effects of soil moisture and dried raindroplet crust on saltation and dust emission. J. Geophys. Res. 113, D24212. doi:10.1029/2008JD009955.
Jickells, T.D., Spokes, L.J., 2001. Atmospheric Iron Inputs to the Oceans. In: Turner, D.R., Hunter, K. (Eds.), The Biogeochemistry of Iron in Seawater SCOR/IUPAC Series. Wiley, pp. 85–121.
Jickells, T.D., An, Z.S., Andersen, K.K., Baker, A.R., Bergametti, G., Brooks, N., Cao, J.J., Boyd, P.W., Duce, R.A., Hunter, K.A., Kawahata, H., Kubilay, N., la Roche, J., Liss, P.S., Mahowald, N., Prospero, J.M., Ridgwell, A.J., Tegen, I., Torres, R., 2005. Global iron connections between dust, ocean biogeochemistry and climate. Science 308, 67–71.
Jilbert, T., Reichart, G.J., Aeschlimann, B., Guntherr, D., Boer, W., de Lange, G., 2010. Climate-controlled multidecadal variability in North African dust transport to the Mediterranean. Geology 38, 19–22.
Jung, E.J., Shao, Y., 2006. An inter-comparison of four wet deposition schemes for dust transport model. Global Planet. Changes 52, 248–260.
Kai, K., Nagata, Y., Tsunematsu, N., Matsumura, T., Kim, H.S., Matsumoto, T., Hu, S.J., Zhou, H.F., Abo, M., Nagai, T., 2008. The structure of the dust layer over the Taklimakan Desert during the dust storm in April 2002 as observed using a depolarization lidar. J. Metoeol. Soc. Japan 86, 1–16.
Kalnay, E., 2003. Atmospheric Modeling, Data Assimilation and Predictability. Cambridge University Press.
Karam, Bou, Flamant, D., Tulet, C., Chaboureau, P., Dabas, J.P., J.P., Todd, M.C., 2009. Estimate of Sahelian dust emissions in the intertropical discontinuity region of the West African Monsoon. J. Geophys. Res. 114, D13106. 10.1029/2008JD011444.
Kaufman, Y.J., Tanré, D., Dubovik, O., Karnieli, A., Remer, L.A., 2001. Absorption of sunlight by dust as inferred from satellite and ground-based remote sensing. Geophys. Res. Lett. 28, 1479–1482.
Kawahata, H., 2002. Shifts in oceanic and atmospheric boundaries in the Tasman Sea (Southwest Pacific) during the Late Pleistocene: evidence from organic carbon and lithogenic fluxes. Palaeogeogr. Palaeoclimatol. Palaeoecol. 184, 225–249.
Kayetha, V.K., Senthil Kumar, J., Prasad, A.K., Cervone, G., Singh, R.P., 2008. Effect of dust storm on ocean color and snow parameters. J. Indian Soc. Remote Sensing 35, 1–9. doi:10.1007/BF02991828.
Kim, S.-W., Choi, I.-J., Yoon, S.-C., 2010. A multiyear analysis of clear-sky aerosol optical properties and direct radiative forcing at Gosan, Korea (2001–2008). Atmos. Res. 95, 279–287.
Klose, M., Shao, Y., Karremann, M.K., Fink, A.H., 2010. Sahel dust zone and synoptic background. Geophys. Res. Lett. doi:10.1029/2010GL042816.
Knippertz, P., Todd, M.C., 2010. The central west Saharan dust hotspot and its relation to African easterly waves and extratropical disturbances. J. Geophys. Res. 115, D12117. doi:10.1029/2009JD012819.
Knippertz, P., Deutscher, C., Kandler, K., Müller, T., Schulz, O., Schütz, L., 2007. Dust mobilization due to density currents in the Atlas region: Observations from the SAMUM 2006 field campaign. J. Geophys. Res. 112, D21109. doi:10.1029/2007JD008774.
Knippertz, P., Ansmann, A., Althausen, D., Muller, D., Tesche, M., Bierwirth, E., Dinter, T., Muller, T., Von Hoyningen-Huene, W., Schepanski, K., Wendisch, M., Heinold, B., Kandler, K., Petzold, A., Schutz, L., Tegen, I., 2009. Dust mobilization and transport in the northern Sahara during SAMUM 2006 - a meteorological overview. Tellus B 61, 12–31. doi:10.1111/j.1600-0889.2008.00380.x.
Kohfeld, K., Harrison, S.P., 2001. DIRTMAP: the geologic record of dust. Earth Sci. Rev. 54, 81–114.
Kohfeld, K., Tegen, I., 2007. Record of mineral aerosols and their role in the Earth system. Treatise Geochem. 4, 1–26.
Kukla, G., 1987. Loess stratigraphy in central China. Quat. Sci. Rev. 6, 191–219.
Kurosaki, Y., Mikami, M., 2005. Regional difference in the characteristics of dust event in East Asia: relationship among dust outbreak, surface wind, and land surface condition. J. Meteorol. Soc. Japan 83A, 1–18.
Lafon, S., Rajot, J.L., Alfaro, S.C., Gaudichet, A., 2004. Assessing the iron-oxides content in desert aerosols. Atmos. Environ. 38, 1211–1218.
Lambert, F., Delmonte, B., Petit, J.R., Bigler, M., Kaufmann, P.R., Hutterli, M.A., Stocker, T.F., Ruth, U., Steffensen, J.P., Maggi, V., 2008. Dust–climate couplings over the past 800,000 years from the EPICA Dome C ice core. Nature 452. doi:10.1038/nature06763: 616-619.
Lavaysse, C., Flamant, C., Janicot, S., Parker, D.J., Lafore, J.-P., Sultan, B., Pelon, J., 2009. Seasonal evolution of the West African heat low: a climatological perspective. Climate Dyn. 33, 313–330. doi:10.1007/s00382-009-9553-4.
Levin, Z., Teller, A., Ganor, E., Yin, Y., 2005. On the Interactions of Mineral Dust, Sea-Salt Particles, and Clouds: A Measurement and Modeling Study from the Mediterranean Israeli Dust Experiment Campaign. J. Geophys. Res. 110, D20202, doi:10.1029/2005JD005810.
Liu, T.S., 1965. The Loess Deposits in China. Sci Press, Beijing (in Chinese).
Liu, T.S. (Ed.), 1985. Loess and the Environment. China Ocean Press, Beijing.
Liu, T.S., Ding, Z.L., Rutter, N., 1999. Comparison of Milankovitch periods between continental loess and deep sea records over the last 2.5 Ma. Quaternary Sci. Rev. 18, 1205–1212.
Liu, L.Y., Shai, P.J., Gao, S.Y., Zou, X.Y., Erdon, H., Yan, P., Li, X.Y., Ta, W.Q., Wang, W.Q., Zhang, C.L., 2004. Dustfall in China's western loess plateau as influenced by dust storm and haze events. Atmos. Environ. 38, 1699–1703.
Liu, Z., Omar, A., Vaughan, M., et al., 2008. CALIPSO lidar observations of optical properties of Saharan dust: A case study of long range transport. J. Geophys. Res. 113, D07207. doi:10.1029/2007JD008878.
Lu, Y.C., Prescott, J.R., Robertson, G.B., Hutton, J.T., 1987. Thermoluminescence dating of the Malan loess at Zhaitang, China. Geology 15, 603–605.
Lu, Y.C., Zhang, J.Z., Xie, J., 1988. Thermoluminescence dating of loess and paleosols from the Lantian section, Shaanxi Province, China. Quaternary Sci. Rev. 7, 245–250.
Lu, Y.C., Wang, X.L., Wintle, A.G., 2007. A new OSL chronology for dust accumulation in the last 130, 000 yr for the Chinese Loess Plateau. Quat. Res. 67, 152–160.
Lunt, D.J., Valdes, P.J., 2001. Dust transport to Dome C, Antarctica, at the Last Glacial Maximum and present day. Geophys. Res. Lett. 28 (2), 295–298.
Luo, C., Mahowald, N.M., del Corral, J., 2003. Sensitivity study of meteorological parameters on mineral aerosol mobilization, transport, and distribution. J. Geophys. Res. 108, 4447. doi:10.1029/2003JD003483.
Mackie, D.S., Boyd, P.W., Hunter, K.A., McTainsh, G.H., 2005. Simulating the cloud processing of iron in Australian dust: pH and dust concentration. Geophys. Res. Lett. 32, L06809. doi:10.1029/2004GL022122.
Mackie, D.S., Boyd, P.W., McTainsh, G.H., Tindale, N.W., Westberry, T.K., Hunter, K.A., 2008. Biogeochemistry of iron in Australian dust: From eolian uplift to marine uptake. Geochem. Geophys. Geosyst. 9. doi:10.1029/2007GC001813.
Maher, B.A., Kohfeld, K., 2009. 'DIRTMAP' Version 3, LGM and late Holocene aeolian fluxes from ice cores, marine sediment traps, marine sediments and loess deposits.Available from: http://www.lec.lancs.ac.uk/dirt.
Maher, B.A., Prospero, J.M., Mackie, D., Gaiero, D., Hesse, P., Balkanski, Y., 2010. Global connections between aeolian dust, climate and ocean biogeochemistry at the present day and at the last glacial maximum. 99, 1–2, 61–97. doi:10.1016/j.earscirev.2009.12.001.
Mahowald, N., Kohfeld, K., Hansson, M., Balkansi, Y., Harrison, S.P., Prentice, I.C., Schulz, M., Rodhe, H., 1999. Dust sources and deposition during the last glacial maximum and current climate: a comparison of model results with paleodata from ice cores and marine sediments. J. Geophys. Res. 104 (D13), 15895–15916.

Mahowald, N., Yosioka, M., Collins, W.D., Conley, A.J., Fillmore, D.W., Coleman, D.B., 2006. Climatic response and radiative forcing from mineral aerosols during the last glacial maximum, pre-industrial, current and double-carbon dioxide climates. Geophys. Res. Lett. 33, L20705. 1029/2006GL026126.

Mahowald, N., Engelstaedter, S., Luo, A., Sealy, A., Artaxo, P., Benitez-Nelson, C., Bonnet, S., Chen, Y., Chuang, P.Y., Cohen, D.D., Dulac, F., Herut, B., Johansen, A.M., Kubilay, N., Losno, R., Maenhaut, W., Paytan, A., Prospero, J.M., Shank, L.M., Siefert, R.L., 2009. Atmospheric iron deposition: Global distribution, variability, and human perturbations. Annu. Rev. Marine. Sci. 2009.1, 245–278.

Marinov, I., Follows, M., Gnanadesikan, A., Sarmiento, J.L., Slater, R.D., 2008. How does ocean biology affect atmospheric pCO_2? Theory and models. J. Geophys. Res. 113, C07032, doi:10.1029/2007JC004598.

Marticorena, B., Bergametti, G., 1995. Modelling the atmospheric dust cycle: 1. Design of a soil-derived dust emission scheme. J. Geophys. Res. 100, 16415–16430.

Marticorena, B., Bergametti, G., Aumont, B., Callot, Y., N'Doume, C., Legrand, M., 1997. Modeling the atmospheric dust cycle: 2 simulation of Saharan dust sources. J. Geophys. Res. 102D, 4387–4404.

Martin, J.H., Fitzwater, S.E., 1988. Iron deficiency limits phytoplankton growth in the north-east Pacific subarctic. Nature 331 (6154), 341–343.

Martínez-Garcia, A., Rosell-Melé, A., Geibert, W., Gersonde, R., Masqué, P., Gaspari, V., Barbante, C., 2009. Links between iron supply, marine productivity, sea surface temperature, and CO_2 over the last 1.1 Ma. Paleoceanography 24, PA1207, doi:10.1029/2008PA001657.

McGowan, H.A., Clark, A., 2008. Identification of dust transport pathways from Lake Eyre, Australia using Hysplit. Atmos. Environ. 42, 6915–6925.

McGowan, H.A., McTainsh, G.H., Zawar-Reza, P., 2000. Identifying regional dust transport pathways: application of kinematic trajectory modelling to a trans-Tasman case. Earth Surf. Proc. Landforms 25, 633–647.

McTainsh, G.H., 1989. Quaternary aeolian dust processes and sediments in the Australian region. Quaternary Sci. Rev. 8, 235–253.

McTainsh, G.H., 1998. Dust storm index. In: Sustainable Agriculture: Assessing Australia's Recent Performance. a Report of the National Collaborative Project on Indicators for Sustainable Agriculture. SCARM Technical Report 70, 65–72.

McTainsh, G.H., 1999. Dust transport and deposition. In Goudie, A.S., Livingstone, I., Stokes, S. Aeolian Environments, Sediments and Landforms. John Wiley Sons, U.K. Chapter 9, pp. 181–211.

McTainsh, G.H., Leys, J.F., 1993. Chapter 7 – Wind erosion. In GH McTainsh and WC Boughton (Eds) Land Degradation Processes in Australia. Longman-Cheshire, pp. 188–233.

McTainsh, G.H., Pitblado, J.R., 1987. Dust storms and related phenomena measured from meteorological records in Australia. Earth Surf. Proc. Landforms 12, 415–424.

McTainsh, G.H., Strong, C., 2007. The role of aeolian dust in ecosystems. Geomorphology – Special Issue on Geomorphology and Ecosystems. 89 91-2, pp. 39–54.

McTainsh, G.H., Chan, Y.C., McGowan, H., Leys, J.F., Tews, K., 2005. The 23rd October 2002 dust storm in eastern Australia: Characteristics and meteorological conditions. Atmos. Environ. 39(7), 1227–1236, doi:10.1016/j.atmosenv.2004.10.016.

Menut, L., 2008. Sensitivity of hourly Saharan dust emissions to NCEP and ECMWF modeled wind speed, J. Geophys. Res. 113, D16201, doi:10.1029/2007JD009522.

Menut, L., Chiapello, I., Moulin, C., 2009. Predictability of mineral dust concentrations: The African Monsoon Multidisciplinary Analysis first short observation period forecasted with CHIMERE-DUST. J. Geophys. Res. 114, D07202, doi:10.1029/2008JD010523.

Meskhidze, N. et al., 2005. Dust and pollution: a recipe for enhanced ocean fertilization? J. Geophys. Res. 110. doi:10.1029/2004JD005082.

Miller, R., Tegen, I., Perlwitz, Z., 2004. Surface radiative forcing by soil dust aerosols and the hydrologic cycle. J. Geophys. Res. 109, D04203, doi:10.1029/2003JD004085.

Moreno, A., Cacho, I., Canals, M., Prins, M.A., Sànchez-Goñi, M.F., Grimalt, J.O., Weltje, G.J., 2002. Saharan dust transport and high-latitude glacial climatic variability: the Alboran sea record. Quaternary Res. 58, 318–328.

Nakajima, T., Sekiguchi, M., Takemura, T., Uno, I., Higurashi, A., Kim, D., Sohn, B.J., Oh, S-N, Nakajima, T.Y., Ohta, S., Okada, I., Takemura, T., Kawamoto, K., 2003. Significance of direct and indirect radiative forcings of aerosols in the East China Sea region. J. Geophys. Res. 108, 8658, doi:10.1029/2002JD003261.

Nakajima, T., Yoon, S-C, Ramanathan, V., Shi, G.Y., Takemura, T., Higurashi, A., Takamura, T., Aok, K., Sohn, B-J, Kim, S-W, Tsuruta, H., Sugimoto, N., Shimizu, A., Tanimoto, H., Sawa, Y., Lin, N-H, Lee, C-T, Goto, D., Schutgens, N., 2007. Overview of the Atmospheric Brown Cloud East Asian Regional Experiment 2005 and a study of the aerosol direct radiative forcing in east Asia. J. Geophys. Res. 112, D24S91. doi:10.1029/2007JD009009.

Nickovic, S., Dobricic, S., 1996. A model for long-range transport of desert dust. Mon. Weather Rev. 124, 2537–2544.

O'Loingsigh, T., McTainsh, G.H., Tapper, N.J., Shinkfield, P., 2010. Lost in code: a critical analysis of using meteorological data for wind erosion monitoring. Aeolian Res. 2, 49–57.

Pérez, C., Nickovic, S., Pejanovic, G., Baldasano, J.M., Özsoy, E., 2006.. J. Geophys. Res. 111, D16206, doi:10.1029/2005JD006717.

Perlwitz, J., Tegen, I., Miller, R.L., 2001. Interactive soil dust aerosol model in the GISS GCM: 1. Sensitivity of the soil dust cycle to radiative properties of soil dust aerosols. J. Geophys. Res. 106, 18167-18192, doi:10.1029/2000JD900668.

Peterson, S.T., Junge, C.E., 1971. Sources of particulate matter in the atmosphere. In Kellog WW, GD Robinson (eds) Man's Impact on the Climate. MIT Press 310-320.

Pettke, T., Halliday, A.N., Rea, D.K., 2002. Cenozoic evolution of Asian climate and sources of pacific seawater Pb and Nd derived from eolian dust of sediment core LL44-GPC3. Paleoceanography 17(3) 1031. 10.10290/2001PA000673.

Pilinis, C., Seinfeld, J.H., 1987. Continued development of a general equilibrium model for inorganic multicomponent atmospheric aerosols. Atmos. Envion. 21, 2453–2466.

Porter, S.C., An, Z., 1995. Correlation between climate events in the North Atlantic and China during the last glaciation. Nature 375, 305–308.

Prospero, J.M., 1999. Long-range transport of mineral dust in the global atmosphere: Impact of African dust on the environment of the southeastern United States. Proc. Natl. Acad. Sci. 96, 3396–3403.

Prospero, J.M., Ginoux, P., Torres, Q., et al., 2002. Environmental characterization of global sources of atmospheric soil dust identified with the Nimbus 7 Total Ozone Mapping Spectrometer (TOMS) absorbing aerosol product. Rev. Geophys. 1, 1–22.

Pudmenzky, C., Butcher, A.R., Cropp, A., McTainsh, G.H., 2006. How QEMSCAN^{TM} technology can contribute to an understanding of the possible climate impacts of atmospheric dust. Minerals Engineering Conference – Automated Mineralogy 06, Brisbane, Australia, 2006.

Pye, K., 1984. Loess. Progr. Phys. Geogr. 8, 176–215.

Qin, X., Mu, Y., Ning, B., Yin, Z., 2009. Climate effects of dust aerosols in southern Chinese Loess Plateau over the last 140,000 years. Geophys. Res. Lett. 36, L02707, doi:10.1029/2008Gl036156.

Quijano, A.L., Sokolik, I., Toon, O.B., 2000. Radiative heating rates and direct radiative forcing by mineral dust in cloudy atmospheric conditions. J. Geophys. Res. 105, 12,207-12,219.

Ramaswamy, V., Boucher, O., Haigh, J., Hauglustaine, D., Haywood, J., Myhre, G., Nakajima, T., Shi, G.Y., Solomon, S., 2001: Radiative forcing of climate change, in climate change, The Scientific Basis, Contribution of Working Group I to Third Assessment Report of the Intergovernmental Panel on Climate Change (eds. Houghton JT, Y Ding, DJ Griggs et al.), New York, Cambridge Univ. Press, 349-416.

Ramos, A.G., Cuevas, E., Perez, C., Baldasano, J.M., Coca, J., Redondo, A., Alonso-Perez, S., Bustos, J.J., Nickovic, S., 2008: Saharan Dust and Bloom of Diazotrophic Cyanobacteria in the NW African Upwelling. In: European Geoscience Union (EGU) General Assembly. Vienna, April 13-18.

Raupach, M.R., Lu, H., 2004. Representation of land-surface processes in Aeolian transport models. Environm Mod. Software 19, 93–112.

Rea, D.K., 1994. The paleoclimatic record provided by eolian deposition in the deep sea: the geologic history of wind. Rev. Geophys. 32, 159.

Rea, D.K., Snoechx, H., Joseph, L.H., 1998. Late Cenozoic eolian deposition in the North Pacific: Asian drying, Tibetan uplift, and cooling of the northern hemisphere. Paleoceanography 13, 215–224.

Reader, M.C., Fung, I., McFarlane, N., 1999. The mineral dust aerosol cycle during the Last Glacial maximum. J. Geophys. Res. 104 (D8), 9381–9398.

Reinfried, F., Tegen, I., Heinold, B., Hellmuth, O., Schepanski, K., Cubasch, U., Huebener, H., Knippertz, P., 2009. Simulations of convectively-driven density currents in the Atlas region using a regional model: Impacts on dust emission and sensitivity to horizontal resolution and convection schemes. J. Geophys. Res. 114, D08127, doi:10.1029/2008JD010844.

Richthofen, F., 1877: China I. Berlin.

Richthofen, F., 1882. On the mode of origin of the loess. Geological Magazine 9, 293–305.

Ruddiman, W.F., 2007. The early Anthropogenic hypothesis: challenges and responses. Rev. Geophys. 45RG4001, doi:10.1029/2006RG00207.

Schepanski, K., Tegen, I., Todd, M.C., Heinold, B., Bönisch, G., Laurent, B., Macke, A., 2009. Meteorological processes forcing Saharan dust emission inferred from MSG-SEVIRI observations of subdaily dust source activation and numerical models. J. Geophys. Res. 114, D10201, doi:10.1029/2008JD010325.

Schmittner, A., Galbraith, E.D., 2008. Glacial greenhouse-gas fluctuations controlled by ocean circulation changes. Nature 456 (7220), 373.

Schulz, M., Balkanski, Y.J., Guelle, W., Dulac, F., 1998. Role of aerosol size distribution and source location in a three-dimensional simulation of a Saharan dust episode tested against satellite-derived optical thickness. J. Geophys. Res. 103, 10579–10592.

Seinfeld, J.H. et al., 2004. ACE-ASIA: regional climatic and atmospheric chemical effects of Asian dust and pollution. Bull. Am. Meteorol. Soc. 85, 367–380.

Sekiyama, T.T., Tanaka, T.Y., Shimizu, A., Miyoshi, T., 2010. Data assimilation of CALIPSO aerosol observations. Atmos. Chem. Phys. 10, 39–49.

Sellers, W.D., 1969. A global climatic model based on the energy balance of the Earth-atmosphere system. J. Appl. Meteorol. 8392-8400.

Shao, Y., 2004. Simplification of a dust emission scheme and comparison with data. J. Geophys. Res. 109, D10202, doi:10.1029/2003JD004372.

Shao, Y., 2008. Physics and modelling of wind erosion. Springer Verlag.

Shao, Y., Dong, C.H., 2006. A review on East Asian dust storm climate, modelling and monitoring. Global Planet. Change 52, 1–22.

Shao, Y., Leslie, L.M., 1997. Wind erosion prediction over the Australian continent. J. Geophy. Res. 102, 30,091-30,105.

Shao, Y., Raupach, M.R., Flindlater, P.A., 1993. Effect of saltation on the entrainment of dust by wind. J. Geophys. Res. 98, 12719–12726.

Shao, Y., Yang, Y., Wang, J.J., Song, Z.X., Leslie, L.M., Dong, C.H., Zhang, S.H., Lin, Z.H., Kanai, Y., Yabuki, S., Chun, Y.S., 2003. Real-time numerical prediction of northeast Asian dust storms using an integrated modeling system. J. Geophys. Res. 108, 4691, 10.1029/2003JD003667.

Shao, Y., Leys, J.F., McTainsh, G.H., Tews, K., 2007. Numerical simulation of the October 2002 dust event in Australia. J. Geophys. Res. 112, D08207, doi:10.1029/2006JD007767.

Shao, Y., Fink, A.H., Klose, M., 2010. Numerical simulation of a continental-scale Saharan dust event. J. Geophys. Res. doi:10.1029/2009JD012678.
Slinn, S.A., 1982. Predictions for particle deposition to vegetative canopies. Atmos. Environ. 16, 1785–1794.
Sokolik, I.N., Toon, O.B., Bergstrom, R.W., 1998. Modeling of radiative characteristics of airborne mineral aerosols at infrared wavelengths. J. Geophys. Res. 103, 8813–8826.
Steffen, W. et al. (Eds.), 2004. Global Change and the Earth System. Springer, Berlin.
Stein, R., Robert, C., 1986. Silicilastic sediments at Sites 588, 590 and 591: Neogene evolution in the southwest Pacific and Australian Climate. In: Kennett, J.P. and von der Borsch, C.C. (eds.), Initial report of the Deep Sea Drilling Project, 90. United States Government Printing Office: 1437-1455.
Stevens, T., Armitage, S.J., Lu, H.Y., Thomas, D.S.G., 2006. Sedimentation and diagenesis of Chinese loess: Implications for the preservation of continuous, high-resolution climate records. Geology 34, 849–852. doi:10.1130/G22472.1.
Stuiver, M., Grootes, P.M., 2000. GISP2 Oxygen isotope ratios. Quat. Res. 53, 277–284.
Su, J., Huang, J., Fu, Q., Minnis, P., Ge, J., Bi, J., 2008. Estimation of Asian dust aerosol effect on cloud radiation forcing using Fu-Liou radiative model and CERES measurements. Atmos. Chem. Phys. 8, 2763–2771.
Sugden, D.E., McCulloch, R.D., Bory, A.J.M., Hein, A.S., 2009. Influence of Patagonian glaciers on Antarctic dust deposition during the last glacial period. Nat. Geosci. 2, 281–285.
Sugimoto, N., Uno, I., Nishikawa, M., Shimizu, A., Matsui, I., Dong, X., Chen, Y., Quan, H., 2003. Record heavy Asian dust in Beijing in 2002: Observations and model analysis of recent events. Geophys. Res. Lett. 30, 1640, doi:10.1029/2002GL016349.
Sugimoto, N., Shimizu, A., Matsui, I., Dong, X., Zhou, J., Bai, X., Zhou, J., Lee, C.H., Yoon, S-C, Okamoto, H., Uno, I., 2006. Network observations of Asian dust and air pollution aerosols using two-wavelength polarization lidars. 23rd International Laser Radar Conference, Nara, Japan, 851–854.
Sun, Y., Wang, X., Liu, Q., Clemes, S.C., 2010. Impact of post-depositional processes on rapid monsoon signals recorded by the last glacial deposits of northern China. Earth Planet. Sci. Lett. 289, 171–179.
Svensson, A., Biscaye, P.E., Grousset, F.E., 2000. Characterization of late glacial dust in the Greenland Ice Core Project ice core. J. Geophys. Res. 105 D4, 4637-4656.
Takemura, T., Okamoto, H., Maruyama, Y., Numaguti, A., Higurashi, A., Nakajima, T., 2000. Global three-dimensional simulation of aerosol optical thickness distribution of various origins, J. Geophys. Res. 105 (D14), 17853–17873. doi:10.1029/2000JD900265.
Tanaka, T.Y., Chiba, M., 2006. A numerical study of the contributions of dust source regions to the dust source regions to the global dust budget. Global Planet. Change 52, 88–104.
Taylor, St. R., McLennan, S.M., 1985. The Continental Crust: its Composition and Evolution. Blackwell Scientific Publications.
Tegen, I., Fung, I., 1994. Modeling of mineral dust in the atmosphere: sources, transport, and optical thickness. J. Geophys. Res. 99, 22897–22914.
Tegen, I., Fung, I., 1995. Contribution to the atmospheric mineral aerosol load from land surface modification. J. Geophys. Res. 100, 18707–18726.
Tegen, I., Harrison, S.P., Kohfeld, K., Prentice, I.C., Coe, M., Heimann, M., 2002. Impact of vegetation and preferential source areas on global dust aerosol: Results from a model study. J. Geophys. Res. 107, 4576,doi:10.1029/2001JD000963.
Tegen, I., Werner, M., Harrison, S.P., Kohfeld, K.E., 2004. Relative importance of climate and land use in determining present and future global soil dust emission. Geophys. Res. Lett. 31, L05105, doi:10.1029/2003GL019216.
Textor, C., Schulz, M., Guibert, S., Kinne, S., Balkanski, Y., Bauer, S., Berntsen, T., Berglen, T., Boucher, O., Chin, M., Dentener, F., Diehl, T., Easter, R., Feichter, H., Fillmore, D., Ghan, S., Ginoux, P., Gong, S., Grini, A., Hendricks, J., Horowitz, L., Huang, P., Isaksen, I., Iversen, T., Kloster, S., Koch, D., Kirkevag, A., Kristjansson, J.E., Krol, M., Lauer, A., Lamarque, J.F., Liu, X., Montanaro, V., Myhre, G., Penner, J., Pitari, G., Reddy, S., Seland, Ø., Stier, P., Takemura, T., Tie, X., 2006. Analysis and quantification of the diversities of aerosol life cycles within AeroCom. Atmos. Chem. Phys. 6, 1777–1813.
Textor, C., Schulz, M., Guibert, S., Kinne, S., Balkanski, Y., Bauer, S., Berntsen, T., Berglen, T., Boucher, O., Chin, M., Dentener, F., Diehl, T., Feichter, H., Fillmore, D., Ginoux, P., Gong, S., Grini, A., Hendricks, J., Horowitz, L., Huang, P., Isaksen, I., Iversen, T., Kloster, S., Koch, D., Kirkevag, A., Kristjansson, J.E., Krol, M., Lauer, A., Lamarque, J.F., Liu, X., Montanaro, V., Myhre, G., Penner, J., Pitari, G., Reddy, S., Seland, Ø., Stier, P., Takemura, T., Tie, X., 2007. The effect of harmonized emissions on aerosol properties in global models–an AeroCom experiment. Atmos. Chem. Phys. 7, 4489–4501.
Thiede, J., 1979. Wind regimes over the late Quaternary southwest Pacific Ocean. Geology 7, 259–262.
Thompson, L., Yao, T., Davis, M.E., Henderson, K.A., Mosley-Thompson, E., Lin, P.N., Beer, J., Synal, H.A., Cole-Dai, J., Bolzan, J.F., 1997. Tropical climate instability: the Last Glacial Cycle from a Qinghai-Tibetan ice core. Science 276, 1821–1825.
Timmreck, C., Schulz, M., 2004. Significant dust simulation differences in nudged and climatological operation mode of the AGCM ECHAM. J. Geophys. Res. 109, D13202, doi:10.1029/2003JD004381.
Todd, M.C. et al., 2008. Quantifying uncertainty in estimates of mineral dust flux: An intercomparison of model performance over the Bodélé Depression, northern Chad. J. Geophys. Res. 113, D24107, doi:10.1029/2008JD010476.
Tompkins, A.M., Cardinali, C., Morcrette, J-J, Rodwell, M., 2005. Influence of aerosol climatology on forecasts of the African Easterly Jet. Geophys. Res. Lett. 32, L10801, doi:10.1029/2004GL022189.
Uematsu, M., Duce, R.A., Prospero, J.M., 1985. Deposition of atmospheric mineral particles in the North Pacific Ocean. J. Atmos. Chem. 3, 123–138.
Uno, I., Harada, K., Satake, S., Hara, Y., Wang, Z., 2005. Meteorological characteristics and dust distribution of the Tarim Basin simulated by the nesting RAMS/CFORS dust model. J. Meteorol. Soc. Japan 83A, 219–239.
Uno, I., Wang, Z., Chiba, M., Chun, Y.S., Gong, S.L., Hara, Y., Jung, E., Lee, S.S., Liu, M., Mikami, M., Music, S., Nickovic, S., Satake, S., Shao, Y., Song, Z., Sugimoto, N., Tanaka, T., Westphal, D.L., 2006. Dust model intercomparison DMIP study over Asia: overview. J. Geophys. Res. 111, D12213, doi:10.1029/2005JD006575.
Uno, I., Eguchi, K., Yumimoto, K., Takemura, T., Shimizu, A., Uematsu, M., Liu, Z., Wang, Z., Hara, Y., Sugimoto, N., 2009. Asian dust transport one full circuit around the globe. Nature Geoscience 20, 557–560. doi:10.1038/NGEO583.
Vogel, B., Hoose, C., Vogel, H., Kottmeier, C., 2006. A model of dust transport applied to the Dead Sea area. Meteorologische Zeitschrift 15, 611–624.
Wagenbach, D., Preunkert, S., Schafer, J., Jung, W., Tomadin, L., 1996. Northward transport of Saharan dust recorded in a deep Alpine ice core. In: Guerzoni S, R Chester (eds): The impact of African dust across the Mediterranean. Kluwer Academic Publishers, 291-300.
Werner, M., Tegen, I., Harrison, S.P., Kohfeld, K.E., Prentice, I.C., Balkanski, Y., Rodhe, H., Roelandt, C., 2002. Seasonal and interannual variability of the mineral dust cycle under present and glacial climate conditions. J. Geophys. Res. 107, 4744, doi:10.1029/2002JD002365.
Westphal, D.L., Toon, O.B., Carson, T.N., 1988. A case study of mobilisation and transport of Saharan dust. J. Atmos. Sci. 45, 2145–2175.
Winckler, G., Anderson, R.F., Fleisher, M.Q., McGee, D., Mahowald, N., 2008. Covariant glacial-interglacial dust fluxes in the equatorial Pacific and Antarctica. Science 320, 93–96.
Won, J.-G., Yoon, S.-C., Kim, S.-W., Jefferson, A., Dutton, E.G., Holben, B.N., 2004. Estimation of direct radiative forcing of Asian dust aerosols with sun/sky radiometer and lidar measurements at Gosan, Korea. J. Meteor. Soc. Japan 82, 115–130.
Yamada, Y., Mikami, M., Nagashima, H., 2002. Dust particle measuring system for streamwise dust flux. J. Aird Land Studies 11, 229–234.
Yin, Y., Chen, L., 2007. The effects of heating by transported dust layers on cloud and precipitation: a numerical study. Atmos. Chem. Phys. 7, 3497–3505.
Yoon, S.-C., Won, J.-G., Omar, A.H., Kim, S.-W., Sohn, B.-J., 2005. Estimation of the radiative forcing by key aerosol types in worldwide locations using a column model and AERONET data. Atmos. Environ. 39, 6620–6630.
Yuan, W., Zhang, J., 2006. High correlations between Asian dust events and biological productivity in the western North Pacific. Geophys. Res. Lett. 33, L07603, doi:10.1029/2005GL025174.
Yumimoto, K., Uno, I., Sugimoto, N., Shimizu, A., Liu, Z., Winker, D.M., 2008. Adjoint inversion modeling of Asian dust emission using lidar observations. Atmos. Chem. & Phys. 8, 2869–2884.
Zender, C.S., Bian, H., Newman, D., 2003. Mineral dust entrainment and deposition (DEAD) model: description and 1990s dust climatology. J. Geophys. Res. 108(D14), 4416, doi:10.1029/2002JD002775.
Zhang, D., 2008. Effect of sea salt on dust settling to the ocean. Tellus 60, 641–646.
Zhang, X.Y., Arimoto, R., An, Z.S., 1997. Dust emissions from Chinese desert sources linked to variations in atmospheric circulation. J. Geophys. Res. 102, 28041–28047.
Zhou, Z., 2001. Sand and dusty storm weather of China in recently 45 years. Quat. Res. 21, 9–16.
Zhuang, G., Yi, Z., Duce, R.A., Brown, P.R., 1992. Link between iron and sulfur cycles suggested by detection of iron(II) in remote marine aerosols. Nature 355 (6360), 537–539. 10.1038/355537a0.